4-2013

Development of CFD Models for the Purposes of Exploring Free Surface Wave Phenomena

Leonard P. Stoehr
Western Michigan University, len.stoehr@live.com

DEVELOPMENT OF CFD MODELS FOR THE PURPOSES OF EXPLORING FREE SURFACE WAVE PHENOMENA

by

Leonard P. Stoehr

A Thesis submitted to the Graduate College
in partial fulfillment of the requirements
for the Degree of Master of Science in Engineering (Mechanical)
Department of Mechanical and Aeronautical Engineering
Western Michigan University
April 2013

Thesis Committee:

Parviz Merati, Ph.D., Chair
William W. Liou, Ph.D.
Javier M. Montefort, Ph.D.

DEVELOPMENT OF CFD MODELS FOR THE PURPOSES OF EXPLORING FREE SURFACE WAVE PHENOMENA

Leonard P. Stoehr, M.S.

Western Michigan University, 2013

With the push for finding alternative, green energy sources, the harnessing of energy from ocean and lake waves is becoming a more researched field. To fully understand the behavior of wave interactions and optimize designs to extract this energy, it is necessary to develop computer models that can accurately replicate this behavior. A case is presented in which previous work done using the wave tank found in the Western Michigan University fluids lab is examined. The case involves harnessing the energy generated by ocean waves through the usage of plates of different shapes resting horizontally on the water's surface. The setup and results of the testing are discussed in detail and then the recreated in two dimensions using commercial Computational Fluid Dynamic (CFD) software. The results of the CFD model generated are examined and compared to the experimental data. Efficiency calculations show that while there is potential in the design idea, there may be better means of obtaining this energy. From this a second case is presented in which a three dimensional CFD model is developed demonstrating the behavior of waves impacting a vertical surface, much like a sea wall. The development and results of this model are discussed in detail, and a unique wave phenomenon is identified whereby a corner in the sea wall induces three dimensionality to the system by causing waves to travel parallel to the sea wall.

ACKNOWLEDGMENTS

I would like to thank my advisor Dr. Parviz Merati, for his patience, help and support throughout the long process of this research. I would also like to thank the members of the Western Michigan University Computer Aided Engineering Center, whose support was instrumental to accomplishing my goals.

I would like to thank Dr. William W. Liou and Dr. Javier M. Montefort for taking the time to be members of my master's thesis committee. I would like to thank Rachel A. Durren, whose research and hard work provided the foundation for my master's thesis, as well as for all her support and patience as I strove to understand all of her decisions and processes.

Lastly, I would like to thank my parents, Anne and Len, my sister Kathryn and her fiancé Andrew, as well as the rest of my family for their constant love and support, throughout my entire professional and educational career. Most of all I would like to thank all of them for their eternal patience as they dealt with my sometimes borderline insane behavior and perfectionism throughout the writing of this thesis.

Leonard P. Stoehr

TABLE OF CONTENTS

Table of Contents - continued

LIST OF TABLES

LIST OF FIGURES

List of Figures - continued

1 INTRODUCTION

1.1 Purpose

The idea to use nature's raw power to generate usable work for civilized purposes is not a new concept. Whether it be a windmill, water wheel, or a hydroelectric dam, society has leaned upon forces in nature to assist in the tasks of everyday life. As technology has improved, the means to obtain this energy has changed, and today research is being conducted to harness this energy from ocean and lake waves.

Additionally, the raw processing power that computers contain today is incredible. This power can be used to develop models of ideas, products or behaviors in the hopes that they will give us a better understanding of such items. One such area is that of Computational Fluid Dynamics (CFD), which can be used to model the flow and interaction of fluids with solid bodies or with each other. Applying this simulation method to the area of wave energy capture is a natural step that will be explored in this thesis.

The overall goal was to develop CFD models to aid Western Michigan University with their research into ocean wave energy capture by providing them with a baseline and thought process for how to generate such models. CFD is computationally very challenging, however the everyday computer has reached a point where a simple model can be performed fairly accurately and quickly. This will only improve in the future, therefore providing a method for how to approach such a model is beneficial. Should future research be conducted in this area, the methods used here should allow for a good starting point, but the conditions of any such project should supersede what is recommended here.

1.2 Current CFD Software

Before any CFD models were generated, a determination on the software to be used needed to be made. There are numerous commercial software vendors that produce CFD software that are capable of performing the required functions for the topics explored above. An in depth discussion of each of these is not in the scope of this project, nor would it have much value, as these software programs are updated regularly with new features, performance improvements, etc. However for the purposes of understanding the challenges and the solutions to the problems presented by the developed models, an understanding of the unique capabilities of several of these software packages is valuable. For the purposes of this project, three CFD programs and a meshing program were explored; ANSYS Fluent, ANSYS CFX, and Cradle SC/Tetra. For meshing the models, ICEM was used when necessary.

1.2.1 ANSYS CFX

The ANSYS Corporation currently has two programs capable of CFD in its package. There are several features of CFX that make it appealing to work with. It has very nice integration with the rest of the ANSYS engineering package through the Workbench software, which makes more advanced projects easier to work through, since the importing and exporting of files is taken care of automatically. It also contains the capability to introduce custom code and expressions, albeit in its own programming language. On a lesser note, the layout of the program is very simple to follow and the options are in intuitive locations. The one downside relates to the programs limited options when it comes to the volume of fraction solver method. The method employed by CFX is the same as the Compressive scheme in Fluent. Unlike Fluent however, this is the only method available, and while this method is quite accurate there are some instances in which it is not as favorable, and having the ability to choose the scheme becomes necessary.

1.2.2 Cradle SC/Tetra

The SC/Tetra package is unique in that it contains a combined mesher and solver. It also defaults to using all tetrahedral elements, except where defined around certain bodies or along boundaries. This makes building a model very straightforward. When attempting to recreate the model of the wave tank, the software allows for the assembly of components from individual meshes. So building the wave tank was as simple as creating a meshed tank, a meshed Wave Generator and a meshed Wing and then overlay them appropriately and defining their motion. This works quite well, however when modeling 2D motion this can prove problematic. When generating 2D models a symmetry boundary is used, and should work with moving objects. However what can occur is one of the nodes on the moving objects can move outside the boundaries of the surrounding mesh. This causes the model to fail. The solution is to make the model a 3D model, but this requires significantly more computational power. If the computing resources had been available however, this program would have proven very useful.

1.2.3 ANSYS Fluent

The second product by the ANSYS Corporation designed for CFD is Fluent. Fluent was more recently acquired by the ANSYS group, but the program has been around for many years, and on a fundamental level was designed for research purposes. This means the program has plenty of flexibility, great accuracy, and the capability to introduce custom code segments to augment a simulation. However, the downside is until more recently the program was never optimized to run quickly, so a computer with more processing power and memory is generally required to perform a similar simulation as another CFD program.

The topics explored in this thesis were all done with the use of Fluent. The largest draw was the ability to implement segments of code, and the open channel and wave boundary

conditions. Both of these functions proved very useful and there usage will be explained in detail.

1.3 Research Topics Explored

Two investigations, both involving free surface waves, will be presented in this Thesis. The first project involved the Western Michigan University (WMU) wave tank, found on the engineering campus in their Fluids Laboratory. Prior research involving the wave tank, attempted to harness the energy in waves using plates suspended on the surface (Durren, 2012). For the purposes of comparison, as well as attempting to optimize the shape of the plates on the surface, a 2D CFD model of the WMU wave tank was requested. The model was developed and several simulation runs conducted using various frequencies and plate geometries. Detailed explanations of the model, as well as results compared with data obtained from the wave tank will be presented.

The second project was based around a different concept for harnessing wave energy. The experiments and results from studying flat plates in the WMU wave tank, lead to the desire to study small, high frequency waves impacting vertical walls. A large component of the experimental research conducted at WMU, involved reflecting the generated waves back to the plates using a vertical wall in order to generate larger waves and therefore harness more energy. A look at the CFD results theorized that pressure fluctuations on the vertical wall may also allow for the capture of energy. This project however would require a 3D model, as the previously developed 2D model was incapable of exploring waves impacting the wall at different angles. Detailed explanations of this models creation and its results are presented as well as the identification of a unique phenomenon.

2 WAVE TANK – 2D MODEL

2.1 Project Purpose & Goals

The task provided was to create a CFD model that could accurately represent the WMU wave tank. Additionally it should be capable of obtaining data with which a comparison to the data captured in the wave tank could be compared. The goals of the project then were to develop a CFD model that could accurately represent the previous research conducted in the WMU wave tank, verify it through the comparison of torque data, and ensure the model is simple and flexible enough that it could be easily understood and modified by future researchers using the wave tank.

Ultimately two models were developed, and the results from the models will be compared with experimental data collected previously. The two models share all the same attributes except they differ in their treatment of the behavior of the Wing, as well as several solver settings, but one in particular. These differences will be explored and analyzed in the following sections.

2.2 Model & Simulation Setup

2.2.1 Problem Discussion & Analysis

The dimensions of the full wave tank being modeled for this project can be seen in Figure 2-1. The waves are generated via a small electric motor, attached to a Plexiglas plate which is hinged at the bottom of the tank. Various waves can be generated by adjusting the lever arm mounting point and the speed of the motor. The wing is held in place via an arm attached to another plate on the top of the tank, which is held in place with two C-clamps. Forces on the plate are measured via two calibrated strain gauges.

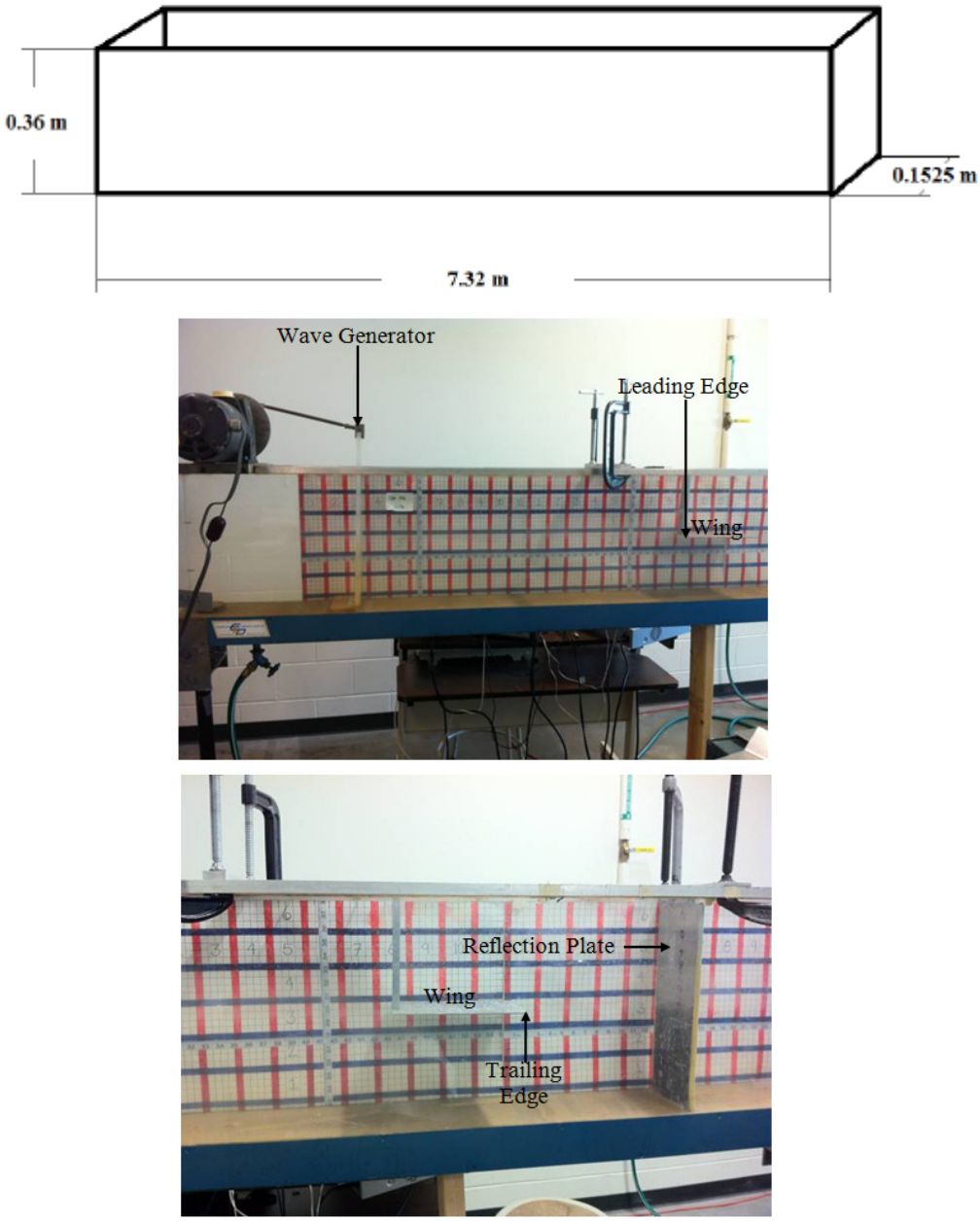

Figure 2.1 Wave tank dimensions and identification of key wave tank features. (*Durren, 2012*)

Pertinent to the model is the fact that the wave tank generates waves that always travel down the length of the tank, and therefore there should be very little change in the waves across the width of the tank. Further the method used to hold the Wing in place, along with the layout and type of strain gauges used, means the data recorded would only be impacted by movement of the plate vertically in the tank; twisting will have a limited effect on the strains

measured. Given this information, the WMU wave tank is a good candidate to be modeled in 2D rather than 3D.

Examining the conditions of the wave tank during which the data was taken, it was found that the two sets of wave parameters were tested (Table 2.1). In addition the wave tank was allowed to run for roughly 10 minutes before data was taken. This was to allow an equilibrium to be reached in the tank in the form of an unchanging standing wave. Another key aspect was the location of the Reflection Plate. The reflection plate shortens the length of the tank and reflects the waves back towards the Wave Generator. This was installed at specific distances to coincide with Nodes and Anti-Nodes. Nodes are points in the standing wave at which no movement occurs, while Anti-nodes are points at which the maximum peak and troughs in the waves occur. The data was gathered via calibrated strain gauges that ultimately allowed the torque to be measured on the Wing. This data was taken, on several different Wing shapes to determine which shape generated the most torque.

Table 2.1 Wave Properties

	Frequency (Hz)	Wavelength (cm)	Amplitude (cm)
Wave 1	0.97	122.3	2.5
Wave 2	1.56	61.2	4.4

From these observations about the experimental data, several decisions could be made as to how the model should be developed. The experimental test data found that the Wave 2 condition produced higher torque values, therefore the model will focus on this wave condition. Additionally, the largest torques for all of the Wing shapes was found when the Reflection plate was placed at an Anti-node. Therefore in the model the Reflection Plate will be placed at the nearest Anti-node beyond the trailing edge of the Wing. This occurs when the distance from the

trailing edge to the Reflection Plate is equal to half the wavelength of the wave being generated. The model will also need to generate a standing wave in the tank, and run a sufficient amount of time to reach an equilibrium. The method for accomplishing this will be discussed further. Because the data collected was converted into torque for comparing the different Wing shapes, this torque will be measured directly from the model, and be used as the defining parameter as to how well the model performs.

2.2.2 Wave Generation

As mentioned previously, there were two models generated, both of which used the same wave generation method. There are several ways to generate waves using Fluent. Fluent uses UDF programs to execute custom functions. In this case a UDF could be written to generate the desired wave profile. Fluent also contains built in functions to generate waves, via the velocity inlet's open wave boundary condition. This function works by specifying a number of the wave characteristics, including the amplitude, wavelength, and phase. Finally the mesh could be designed such that a moving wall, placed at the end or at some point inside the tank could be used to generate the waves.

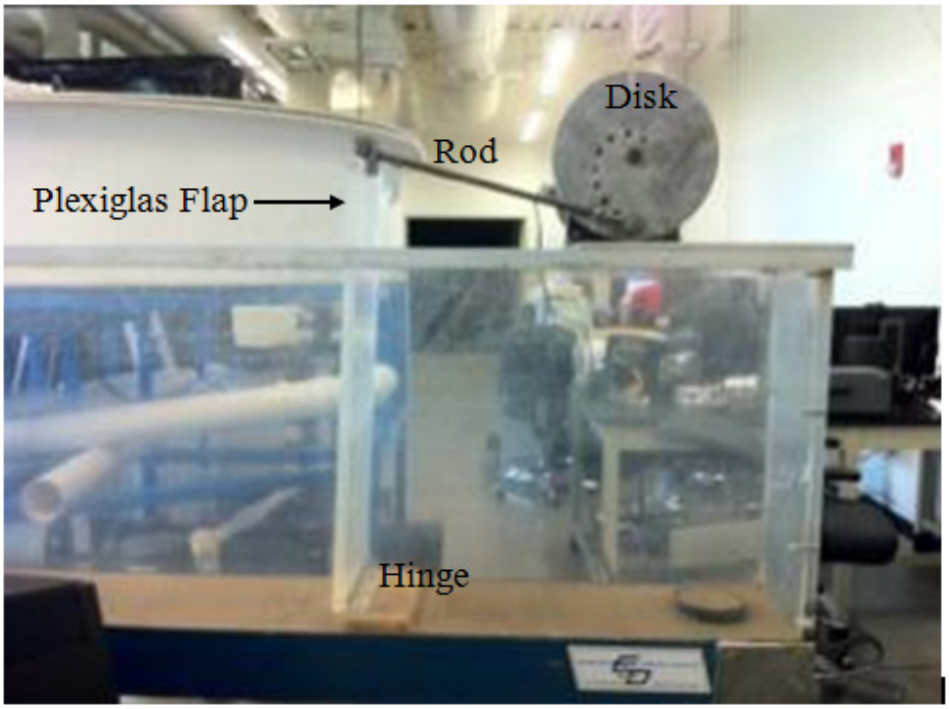

Figure 2.2 Close-up view of the Wave Generator in the wave tank. (*Durren, 2012*)

In this case it was determining to model the Wave Generator as accurately as possible to generate the waves for several reasons. As previously stated, the model needs to be flexible and easy to modify, and by modeling the Wave Generator and using a simple UDF to control the movement, this allows for greater capability and flexibility of the model. Additionally, when the experimental data was taken, the wave conditions were not directly specified; only the Wave Generator specifications were provided. The wave characteristics were obtained by measuring the waves during which the data was acquired. Also one of the overlying goals of the project was to recreate the wave tank, not just the waves, again for flexibility and capability for future projects. Lastly, the experimental data was acquired when a stable standing wave had been generated within the wave tank. The most straight-forward method to accomplish handle all of these concerns is to model the Wave Generator.

Having determined the method with which the waves were to be generated, a closer examination of the Wave Generator was required. It can be observed that Wave Generator is

hinged at the back of the Plexiglas Flap. An examination of the wave tank showed that with the Plexiglas Flap having a vertical starting position. Measurements were taken of the maximum forward and reverse motion, and it was found that the motion was not identical. This would need to be accounted for, as the angle of the plate is key to the size and shape of the waves generated.

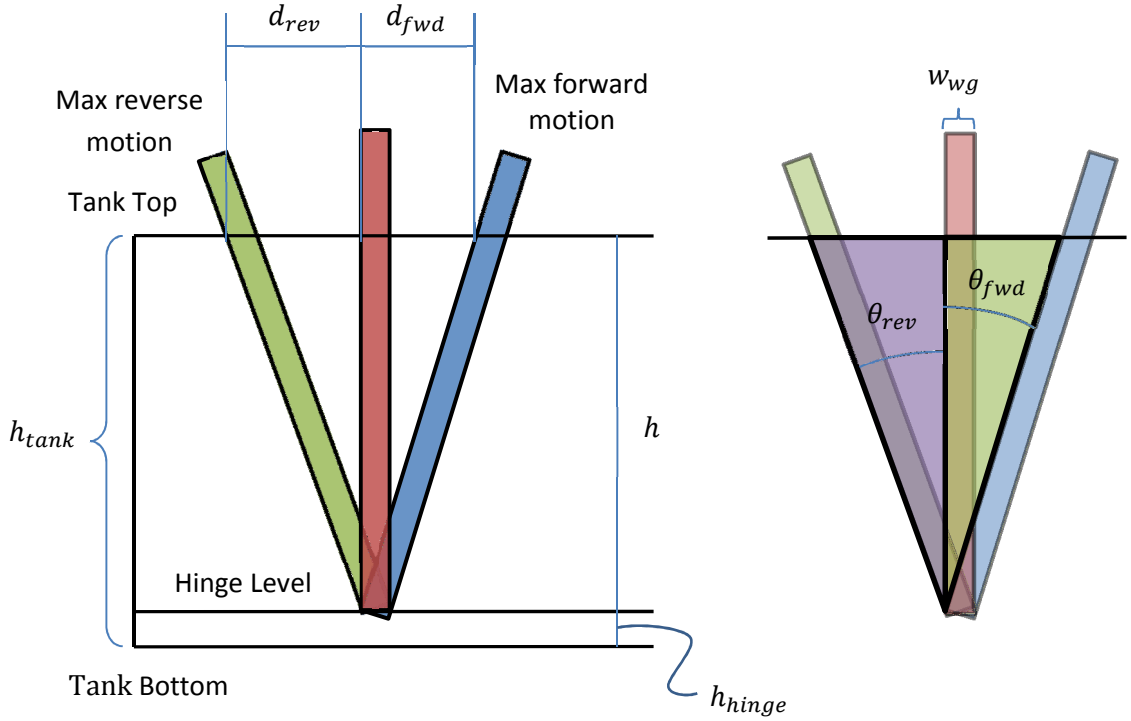

$h_{tank} = 0.360$ m

$h_{hinge} = 0.0127$ m

$h = h_{tank} - h_{hinge} = 0.3473$ m

$d_{fwd} = 0.05837$ m

$d_{rev} = 0.07125$ m

$w_{wg} = 0.0127$ m

$$\theta_{fwd} = \tan^{-1}\left(\frac{d_{fwd}}{h}\right)$$

$$= 11.5936° = 0.2023\ rad$$

$$\theta_{rev} = \tan^{-1}\left(\frac{d_{rev}}{h}\right)$$

$$= 9.5404° = 0.1665\ rad$$

Figure 2.3 Wave Generator measurements and maximum angle calculations

The motion required was implemented via a custom UDF taking advantage of the DEFINE_CG_MOTION macro. This macro allows the specification of the motion of a particular zone, by supplying the velocities, both angular and linear, at every timestep. A single equation can be developed from measurements taken of the wave generator and the frequency of the motion which represents the angular velocity as a function of time. Because the motion of the Wave Generator is not the same in the forward and reverse directions, an equation must be used to account for this. While exploring the usage of SC/Tetra for this project an equation was found within their program that performs this function very well. SC/Tetra describes it as a feathering motion, with the following equation.

$$\theta(t) = A_0 + A_1 \cos(\omega t + \varphi) + B_1 \sin(\omega t + \varphi) \tag{2.1}$$

where A_0, A_1, and A_1 are constants, φ is the phase angle, and the angular frequency ω, is represented by

$$\omega = 2\pi f \tag{2.2}$$

Where f is the frequency in Hertz.

This formula is simply a modified simple harmonic motion, with a phase angle included. While there are likely other equations that are available to model the motion of the Wave Generator, this equation proved very useful as it is extremely flexible, which is one of the keys to this project.

Taking the derivative of equation 2.1,

$$\dot{\theta}(t) = -A_1 \omega \sin(\omega t + \varphi) + B_1 \omega \cos(\omega t + \varphi) \tag{2.3}$$

This is angular velocity as a function of time, which is required by the UDF to define the angular velocity at each timestep. Using the measurements and behavior of the Wave Generator several boundary conditions could be identified.

$$\theta(t = 0) = 0 \tag{2.4}$$

$$\theta\left(t = \frac{1}{4}T = 0.25773\right) = 0.1665 \tag{2.5}$$

$$\theta\left(t = \frac{3}{4}T = 0.77320\right) = -0.2023 \tag{2.6}$$

$$\dot{\theta}\left(t = \frac{1}{4}T = 0.25773\right) = 0 \tag{2.7}$$

Where T is the period equal to the inverse of the frequency.

Between equations 2.1through 2.7, a system of equations can be setup to solve for the unknown variables A_0, A_1, B_1, and φ. Based on the boundary conditions chosen, the following values were obtained.

$$\begin{gathered} A_0 = -0.01791 \\ A_1 = 0.0478 \\ A_2 = -0.1790 \\ \varphi = -2.7836 \end{gathered} \tag{2.8}$$

With a solution found a UDF can be written that allows for any frequency desired to be modeled. The finished UDF can be found in Appendix B.

2.2.3 Boundary Conditions

2.2.3.1 Front

The other boundaries of the both models were also handled in a consistent manner. The front of the tank originally used a wall condition similar to the wave tank was used at first, but this generated a lot of splash, which caused the simulation to slow. Since this area between the wave generator and the front wall provided nothing of useful data or importance in our simulation, the boundary was changed to a pressure outlet, with the open channel boundary condition. This function allows the inflow and outflow of fluid across the boundary at a set fluid depth. In effect, it simulates that fluid extends indefinitely beyond the boundary at the desired depth. In this case when waves were created by the wave generator in the opposite direction from the Wing, they will simply exit the tank instead of being reflected back by a wall, causing considerably less splash. This doesn't completely eliminate returning waves, as when a trough crosses the boundary, the water level is less than then the depth set at the boundary, so water returns from the boundary. However the amount of splash and wave action is greatly reduced, causing solution times to be reduced.

2.2.3.2 Reflection Plate

Mentioned previously, the Reflection Plate's position was key to the behavior of the system. Also as previously mentioned, its location directly influenced the amount of torque the Wing generated. The largets torques were seen when the Reflection Plate was placed at such that an Anti-node were to repeatedly impact the trailing edge of the Wing. This distance from the trailing edge of the Wing to the Reflection Plate was found to be one half the wavelength of the waves being generated. Both models reflected this position. In terms of the boundary

condition, the reflection plate can simply be modeled as a wall boundary. To simplify the model, friction was ignored on the wall, but this could easily be implemented in the future.

2.2.3.3 Top, & Bottom

The top opening of the tank was modeled as a pressure outlet boundary, with the pressure set to a gauge pressure of zero. The bottom was modeled as a no-slip wall, similar to that of the reflection plate.

2.2.4 Wing

The treatment of the Wing is one of the key differences between the two models. The reasoning for modeling it in two ways was to determine whether the Wing could be simplified to the point where it was completely fixed in place. When examining the behavior of the Wing in the wave tank, it was noticed that due to the method in which the Wing was constrained, the Wing moved several centimeters when impacted by the waves. The question then became whether mimicking this motion was necessary or if it could be simplified to the point of being fixed in place. The main advantage with simplifying the model is to increase the speed in which the simulation solved. Additionally it is much easier to implement, and because one of the goals was to create a simple yet accurate and easy to modify model, it is important to determine whether this approach is viable.

Understanding that one of the models had the Wing completely fixed in place, attention can be turned to how to model the Moving Wing. To gain a better understanding of how the Wing should be allowed to move in the simulation, a more careful examination of its behavior in the wave tank was done. It was determined that the appropriate behavior was to treat the leading edge of the Wing as though it's pinned in place, allowing the Wing to rotate freely around this point. To do this, use of the six degree of freedom (6DOF) function was

implemented. The 6DOF function works by providing the desired properties via UDF. These properties include mass, moments and products of inertia, external forces and moments, translational and rotational matrices, and the body constraints. For the problem at hand, the mass, moments of inertia and body constraints were used.

For a flat plate, which is manufactured out of aluminum, calculating the mass and the moments of inertia of the plate can be done with the following equations.

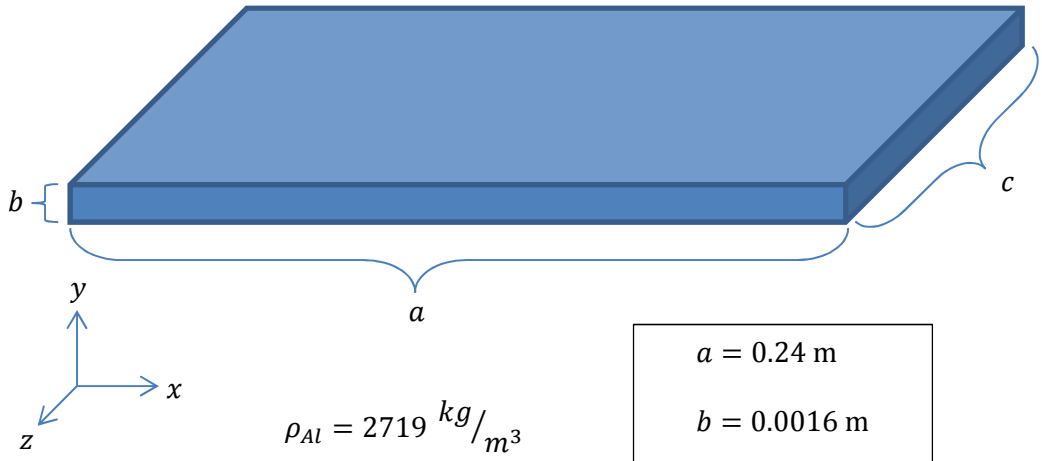

Figure 2.4 Wing Measurements from the WMU Wave Tank

Mass of a Plate:

$$m = \rho(a * b * c) \tag{2.9}$$

Moments of Inertia about Center of Mass:

$$I_{xx} = \frac{1}{12}m(b^2 + c^2) \tag{2.10}$$

$$I_{yy} = \frac{1}{12}m(a^2 + c^2) \tag{2.11}$$

$$I_{zz} = \frac{1}{12} m(a^2 + b^2) \tag{2.12}$$

Parallel Axis Theorem

$$I_s = I_{cm} + md^2 \tag{2.13}$$

Where *d* is the perpendicular distance between center of mass and the axis of rotation.

However, for this particular instance using the calculated values of these would be incorrect. Firstly, because the model is in 2D, rotation around the x-axis and y-axis cannot occur, therefore the values for I_{xx} and I_{yy} are not needed. Secondly, since aluminum is denser than water, this will cause the plate to immediately begin sinking, which is not what happens in our wave tank. The reason this doesn't occur in the wave tank is due to the bar that is supporting the Wing, which is not being modeled. This bar directly impacts the moment of inertia about the z-axis. Additionally, the bar is not the only variable controlling the moment of inertia of the plate. In Figure2.5, it can be seen though that the support device is much more complicated, consisting of multiple bars and two C-clamps. These variables assure that the moment of inertia will be neither constant nor linear in nature. For this case the best way to determine the actual moment of inertia would be to directly measure it. Even this data would be questionable at best because the amount of force being imparted by the C-clamps onto the bar is unknown and would be difficult to reproduce. This all poses a problem as our model requires this information to run.

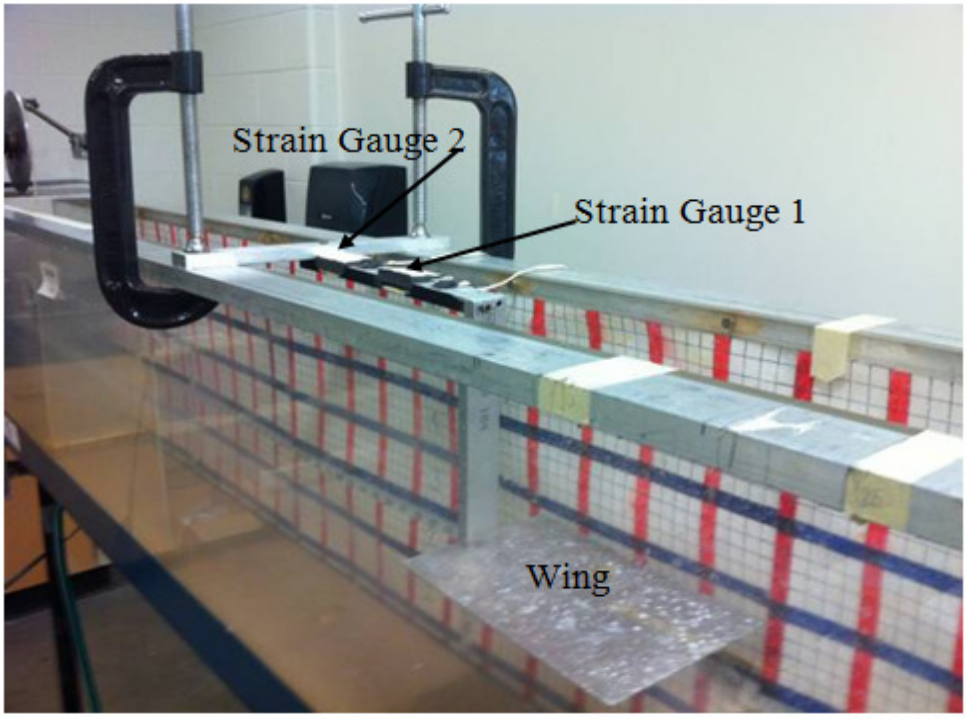

Figure 2.5 Picture of WMU Wave Tank showing the Wing mounting fixtures. (*Durren, 2012*)

In light of this information it helps to reexamine what the goal of the project is. The intent is to create a model that replicates the behavior of the wave tank as accurately as possible in two dimensions. With that in mind it and knowing the experimental data is accurate, we can artificially adjust the values of mass and moment of inertia to achieve our goal. Regarding how to treat the Wing in the model then, the intent is to have the plate float on the surface of the water, with the front of the Wing pinned in place and the motion of the Wing mimic what was seen during the experiments. There are two problems to solve then, how to make the plate float given that the density of the plate is higher than water, and how to allow it to rotate with the correct resistance.

To determine the proper mass for our Wing to remain buoyant, first an understanding of how Fluent handles the z-direction in 2D is required. Fluent assumes everything has a unit length depth; in this case the primary unit of measure is meters, so Fluent assumes everything is

1 meter deep. If it is assumed the object is stationary at the start, then the equation for the mass of an object that is in equilibrium at the surface of a fluid is:

$$m = \rho_f V_{f,disp} \tag{2.14}$$

Where ρ_f is the density of the fluid and $V_{f,disp}$ is the volume of fluid displaced at equilibrium. Therefore if we assume the Wing is submerged half way, then:

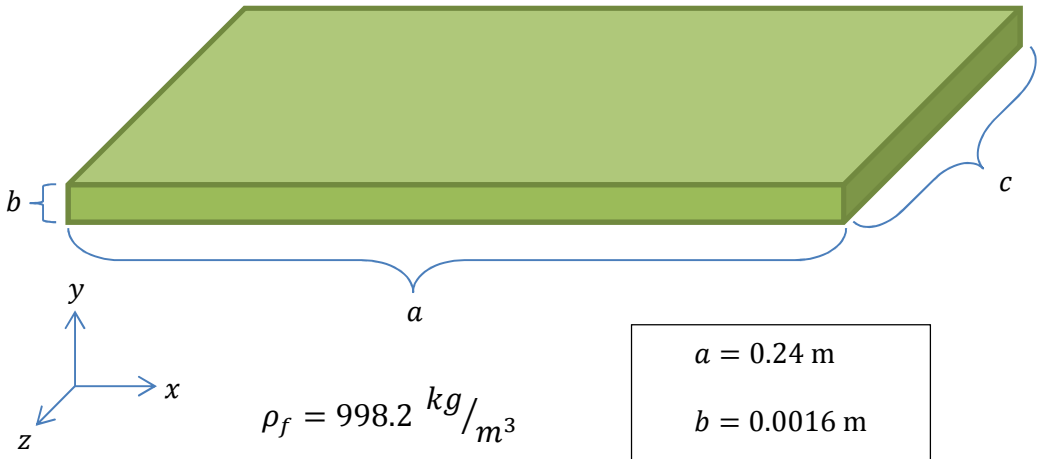

Figure 2.6 Wing Properties as used in the Fixed Wing and Moving Wing Models

$$V_{f,disp} = a * b * c = (0.24)\left(\frac{0.0016}{2}\right)(1) = 1.92 \times 10^{-4}\ \mathrm{m}^3 \tag{2.15}$$

$$m = \rho_f V_{f,disp} = 0.1916544\ \mathrm{kg} \tag{2.16}$$

The determination of the proper moment of inertia was based solely on trial and error. As previously discussed, since the support structure is imparting an unknown amount of resistance to the Wing, running several trial simulations with different moments of inertia was

determined acceptable. The final value found acceptable was determined as $I_z = 0.1\ \mathrm{m}^4$, however this could have been refined further had it been required.

Lastly, there are two body constraints imposed on the Wing. These constraints limit Wing's pinned location such that it cannot move transversely in either the x or y directions.

2.2.5 Mesh

2.2.5.1 Mesh Design

Having discussed how the different segments of the model were handled, the focus can be put on the model's mesh. The meshes of both models were very similar, however several changes needed to be implemented in the Moving Wing model to allow the Wing to behave as desired, therefore the focus will put on its mesh instead of the Fixed Wing model. The mesh, shown in Figure 2.7, is of the Moving Wing model and is broken up into several sections.

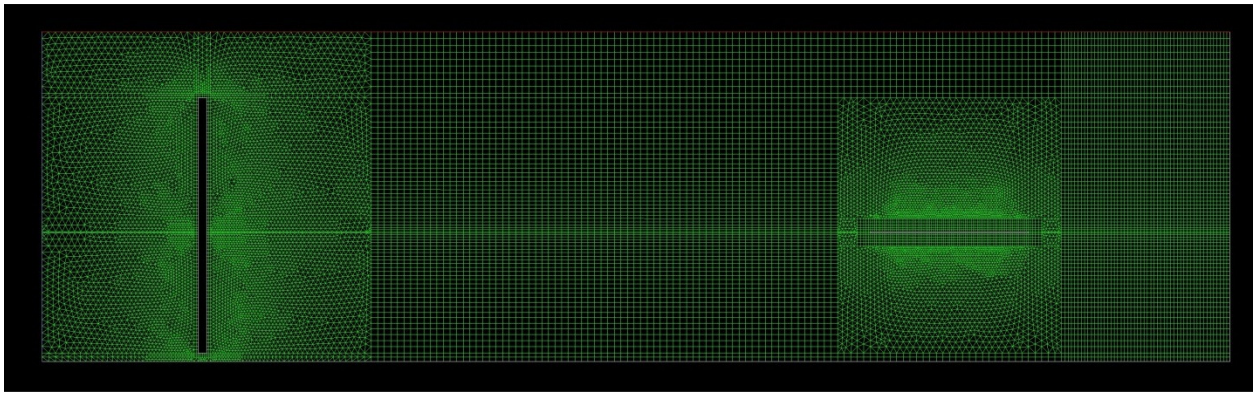

Figure 2.7 Overall view of the mesh for the Moving Wing model

Around each body within the mesh, meaning the wave generator and the wing, a section of fluid exists to move with the body itself. This region is meshed with a very small rectangular or H-grid mesh, and allows for very accurate calculations along the surface and the regions surrounding both bodies (see Figures 2.8 and 2.9). This region also provides for a more stable run and accurate solution. Around each of these regions is a fine tetrahedral or tet mesh.

The dynamic mesh function of Fluent requires a tet mesh for the bodies to move. The other areas, between the wave generator and the wing, and between the wing and the reflection plate, are mesh in a standard H-grid. The H-grid contains less nodes and tends to provide better accuracy for the same mesh size. Meshing these regions in a tet mesh would be acceptable, however the mesh required would need to be smaller resulting in more nodes and lengthening the solution time. Also dividing the mesh up into these regions allows more control over the model, by controlling which regions of the mesh deform. It also makes editing the mesh for changes in geometry easier, as only the sections that are modified will need to be remeshed.

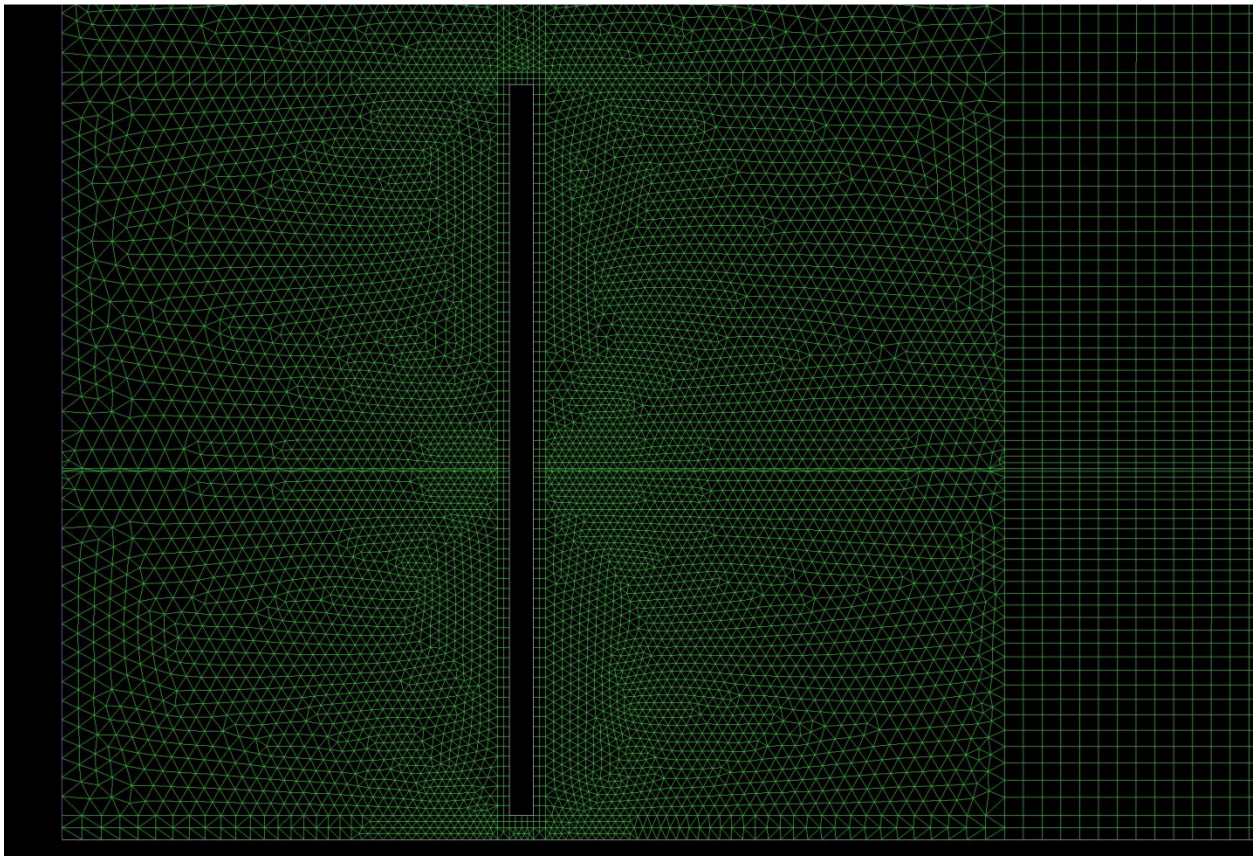

Figure 2.8 Mesh around the Wave Generator, including the H-grid region and the tri-mesh region

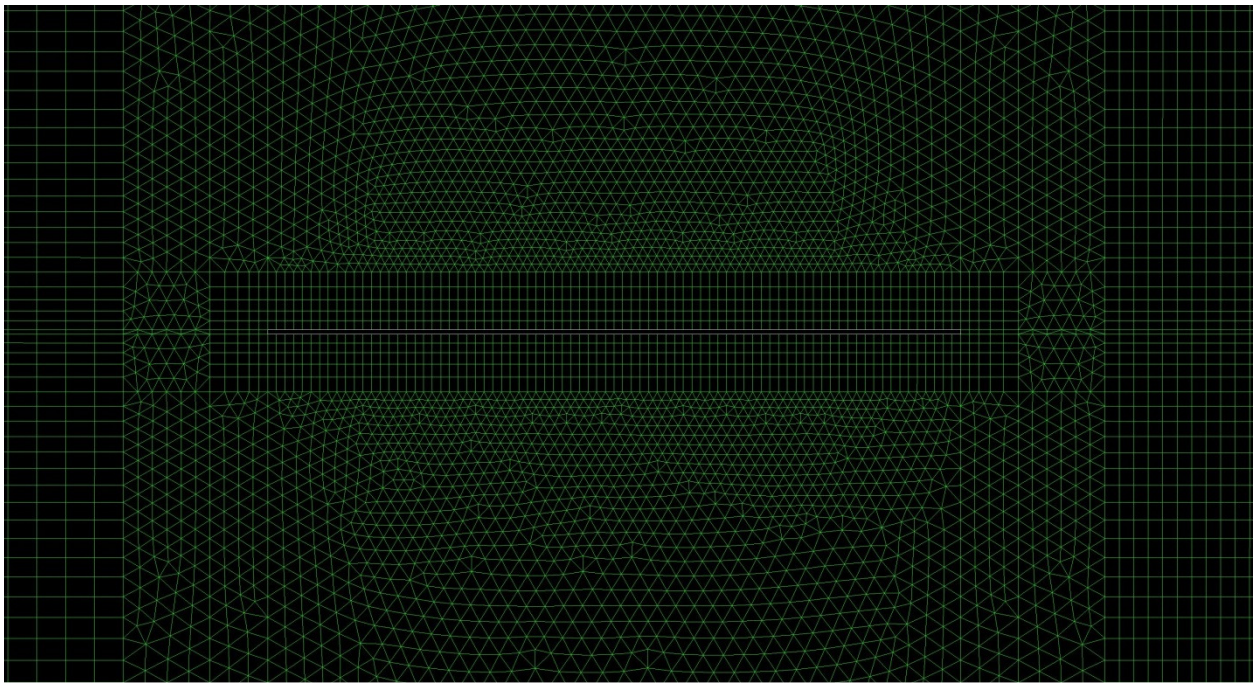

Figure 2.9 Mesh around the Wing of the Moving Wing model

2.2.5.2 Dynamic Mesh Setup

As previously discussed, the method chosen to generate waves in the simulation involves moving the wave generator in a motion mimicking the motion of the actual plate in the WMU wave tank. This is implemented using the dynamic mesh function within Fluent. The dynamic mesh function works by defining a region of the mesh that is allowed to deform. The mesh is then allowed to deform to accommodate the requirements of the UDF controlling the movement of the object. In the case presented here, four regions were defined. Two regions were defined that control the movement of the Wave Generator and the Wing. As discussed earlier, both of these objects are controlled via UDF's that control how the object is allowed to move. In the case of the Wave Generator it's via a function which describes the angular velocity with respect to time, and with the Wing it's floating on the surface and allowed to rotate. The common attribute to both these objects is that they both have a point at which they're allowed to rotate around. From within the dynamic mesh function we can assign the point at which

these objects are fixed, as well as any initial velocities. In this case the initial velocities were all assigned to zero, as it was one of the boundary conditions used to determine the proper coefficients for the Wave Generator motion. The other two regions that are defined are the two H-grid regions surrounding both the bodies. These regions have the same motion as their respective bodies, and must be defined in the same manner. The last option that must be enabled is the 6DOF solver. This option enables the usage of the UDF that defines the physical properties of the Wing. This must be enabled for both the Wing and the meshed region surrounding the Wing. In addition the region surrounding the Wing must have the passive option enabled. This option indicates that the region is not impacted by the external forces, but follows the same motion as the object that is, which in this case is the Wing.

Additionally there are several options within the dynamic mesh control that control how the mesh is modified as the motion takes place. For this project the smoothing and remeshing options were enabled. An additional option is the layering option which was not used.

The smoothing option allows the mesh to stretch and contract. An example of this can be seen in Figure 2.10. The figure shows the mesh around the top of the wave generator at t=0.0 and at t=0.1 seconds. Iterations were performed every 0.001 second, with only the smoothing function enabled. If can clearly be seen that the nodes within the tet mesh have shifted to accommodate the motion of the Wave Generator, while at the same time the nodes within the hex mesh, which is the region that was assigned to move with the Wave Generator, has also shifted but not deformed.

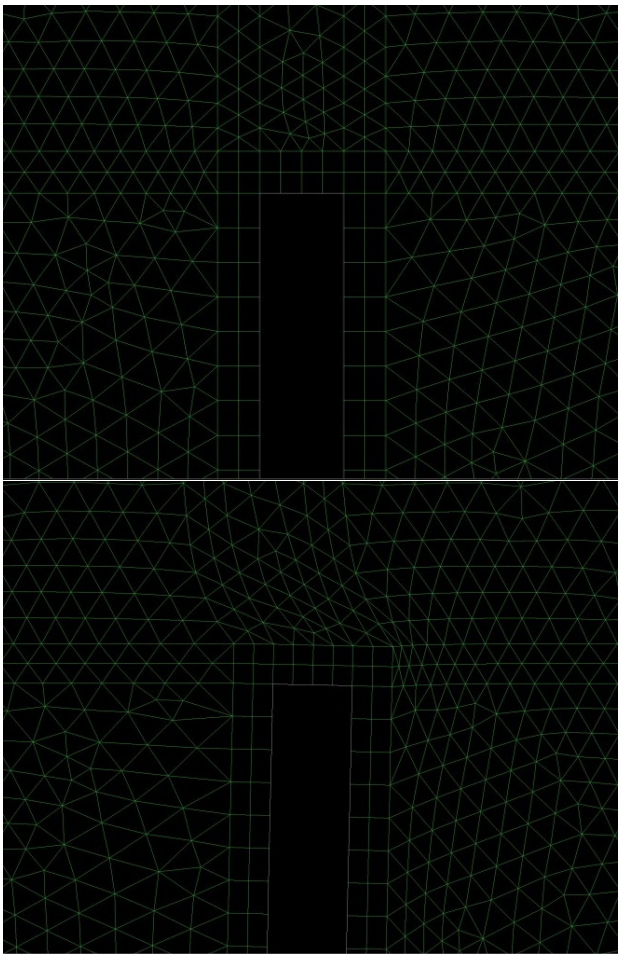

Figure 2.10 Demonstration of the mesh smoothing function, imparted on the meshed regions surrounding the top of the Wave Generator at time t=0 seconds (left) and t=0.1 seconds (right).

This method works well for small body movements; however larger deformations can cause lots of skewed elements, resulting in poor results, and long calculation times. Several of these elements can be seen in the figures as well. The remeshing option helps alleviate these problems by identifying elements of poor quality and remeshing them accordingly. In Figure 2.11, the same motion was generated as previously, but remeshing was enabled. At T=0.1 seconds, it can be seen that several of the skewed elements from previously have been replaced, improving the mesh quality.

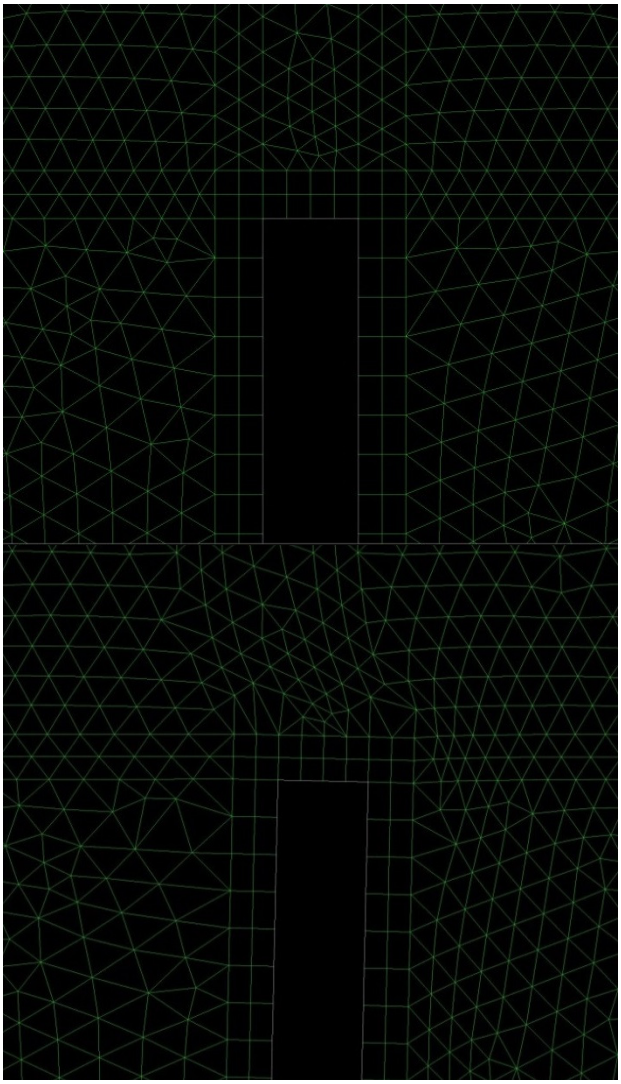

Figure 2.11 Demonstration of the mesh smoothing and remeshing function, imparted on the meshed regions surround the top of the Wave Generator at time t=0 seconds, (left) and t=0.1 seconds (right).

The last option implemented is the Implicit Update function. This option causes the mesh to be updated during each iteration, and not at the beginning. This is useful when the 6DOF solver is used, as the motion of the mesh is directly impacted by the force being imparted on the object by the flow, as is the case with the Wing. Not enabling this solution does not mean the model will not solve or be accurate, however it does increase the robustness of the solution by creating a stronger relationship between the flow and the mesh motion.

2.2.6 Solver Settings

Fluent contains numerous solver controls, many of which can have a large impact on the results. The following discussion revolves around one of the largest differences between the Fixed Wing and Moving Wing models.

2.2.6.1 Multiphase & Volume Fraction

Within the Multiphase section of Fluent, the settings for modeling multiphase flows are found. The model required for this project is the Volume of Fluid (VoF) Model. The VoF model is a surface tracking method that works very well for multiphase flows where a distinct interface is present. This makes the model a very good fit for the present case, as the free surface between the water and air should be well defined and the Wing is located at the interface so high accuracy at the surface is required.

The VoF model assumes that the volume fraction is always between 0 and 1 for a particular phase, meaning there can be no empty regions, and each control volume must be occupied by one or more of the present phases. It contains a single phase continuity equation to solve for the volume fraction and a single set of momentum equations for the entire flow field. It is also capable of handling factors such as surface tension and wall adhesion when enabled, as well as a number of turbulence models.

Within the VoF model there are several options, the most important of which is the VoF Scheme. The VoF Scheme determines how the continuity equation is solved for the volume of fraction of each phase within the solver. In the Explicit scheme, the continuity equation is solved for the volume fractions, and then the volume fraction information is used within the momentum equations, which are then iterated to produce the flow field. The continuity equation is solved in sub-time steps, which occur between the defined timesteps and are based

on the provided Courant number. In the Implicit scheme the continuity equation is iterated with the momentum equation, solving for the volume fraction and flow field at the same time. Both of these methods have advantages and disadvantages. In general, the Explicit Scheme can generate a very clear and accurate interface between the phases and thus works very well with models where surface tension plays a significant role. However it requires a very fine and high quality mesh, and doesn't handle compressible fluids very well. The Implicit scheme doesn't generate as clean of an interface, however it is much more tolerant of meshes containing skewed or poor quality elements and is not limited by the Courant number, and therefore can be run with larger timesteps.

The Fixed Wing model made use of the Explicit Scheme, whilst the Moving Wing model made use of the Implicit Scheme. It was desired to use the Explicit Scheme for both models, however initial trials with the Explicit Scheme proved problematic, and caused model instability and failure. It is believed that this is chiefly due to the mesh used, and could have been corrected if necessary.

Two more options are enabled within the Multiphase settings. The first is the Implicit Body Force option. For models that contain large body forces, such as gravity, the Implicit Body Force function can improve the stability of the model. In this case gravity plays a significant role in the behavior of the Wing, therefore this option should be enabled. The last option enabled in the multiphase settings is the Open Channel function. This function allows for the Open Channel boundary condition that was previously discussed to be enabled. These functions were enabled for both the Fixed Wing and Moving Wing models.

2.2.7 Materials, Phases & Operating Conditions

The materials and their properties used for this are fairly straightforward. Only two fluids were necessary for this project; water in liquid form, and air. Both of these materials were imported with their default properties from the Fluent database.

Fluent uses phases to describe which materials belong to each phase. For this project there are two phases, the primary phase and secondary phase. Fluent assumes that the entire fluid region as defined by the mesh is of the primary phase, unless instructed otherwise. In this case, it's beneficial to assign the primary phase to be air, and the secondary phase to be water.

The operating conditions panel includes the settings for gravity, operating pressure, coordinates for setting the reference pressure location, and the operating density. The gravity setting is straightforward, you assign it to the desired coordinate direction. The reference pressure location sets the location at which the operating pressure is defined. This location should be somewhere in which the pressure is constant throughout the duration of the simulation. The operating pressure is the default pressure at which the system is defined. For this project, the operating pressure is set to 1.0 atmosphere, and the location was set to just off the top outlet, towards the middle of the tank. The operating density should always be set to the lesser density of the fluids being used, in this case air.

2.2.8 Initial Conditions and Solver Settings

To initiate the simulation the water level was set to the same height as the wave tank, with the Wing placed so that the surface of the water is at the midpoint of the Wing's thickness. All other variables including velocity and pressure were set to zero. Using the method discussed Fluent automatically calculates the hydrostatic pressure from the water and applies it when the initial conditions are initialized.

The following is a list comparing the different solver models and spatial discretization schemes used in both the Fixed Wing and Moving Wing models. These schemes determine the accuracy and speed at which the solution is generated. Details on how these schemes work and their appropriateness can be found within the Fluent documentation and therefore will not be repeated here.

Table 2.2 Comparison of solver models for Fixed Wing and Moving Wing models

	Models	
	Multiphase Model	Turbulence
Fixed Wing	Volume of Fluid - Explicit	SST k-ω
Moving Wing	Volume of Fluid - Implicit	Realizable k-ϵ w/ enhanced wall function

Table 2.3 Comparison of solver schemes for Fixed Wing and Moving Wing models

	Schemes						
	Pressure-Velocity Coupling	Gradient	Pressure	Momentum	Volume Fraction	Turbulent Kinetic Energy	Turbulent Dissipation Rate
Fixed Wing	PISO	Least Squares Cell Based	PRESTO!	First Order Upwind	Geo-Reconstruct	First Order Upwind	First Order Upwind
Moving Wing	Coupled	Least Squares Cell Based	PRESTO!	Second Order Upwind	Compressive	Second Order Upwind	Second Order Upwind

The relaxation factors and solution controls can be found tabled below.

Table 2.4 Comparison of Relaxation Factors for the Fixed Wing and Moving Wing models

	Flow Courant Number	Explicit Relaxation Factors	
		Momentum	Pressure
Fixed Wing			
Moving Wing	200	0.5	0.5

	Under-Relaxation Factors								
	Pressure	Density	Body Forces	Momentum	Volume Fraction	Turbulent Kinetic Energy	Specific Dissipation Rate	Turbulent Dissipation Rate	Turbulent Viscosity
Fixed Wing	0.3	1	1	0.5		0.5	0.5		0.5
Moving Wing		0.5	0.5		0.5	0.5		0.5	0.5

The Moving Wing and Fixed Wing models included a final difference which involved how the models were run. Specifically it involved the control of the timestep size. To ensure stability of the Fixed Wing model, which used the Explicit VoF scheme, the variable timestep function was used. The Moving Wing model, could not use this function, and instead was broken into two parts. The first part included very small timesteps to allow the simulation to get running without excessive movement of the mesh, and allow the Wing to more easily adapt to being placed on the water's surface. The second part increased the timestep size to reduce the run time while still maintaining the stability of the model. The following are the criteria used to run the simulation and record the data:

Table 2.5 Breakdown of the run conditions for the Moving Wing model

	Timestep Size (s)	No. of Timesteps	Total Time (s)
Part 1 - Startup	0.001	10	0.01
Part 2 - Running	0.005	8000	40

2.3 Wave Tank Results

2.3.1 Wave Generator Behavior

It is important to first look at the behavior of the Wave Generator in both the Fixed Wing and Moving Wing models before examining how well they perform versus the experimental data. It can be seen that the Wave Generator at 0.64 seconds is very close to the requested 0.641 second period. At t=0.25T, or 0.16 seconds, the Wave Generator is very close to the maximum forward position, and similarly at t=0.75T, or 0.48 seconds, the Wave Generator is very near to the maximum reverse position. Also of note is how the mesh has deformed and been remeshed over the course of a single period. The mesh size has deformed and in areas where the quality was low it was remeshed. Overall the model's Wave Generator motion depicts what was found in the wave tank very well.

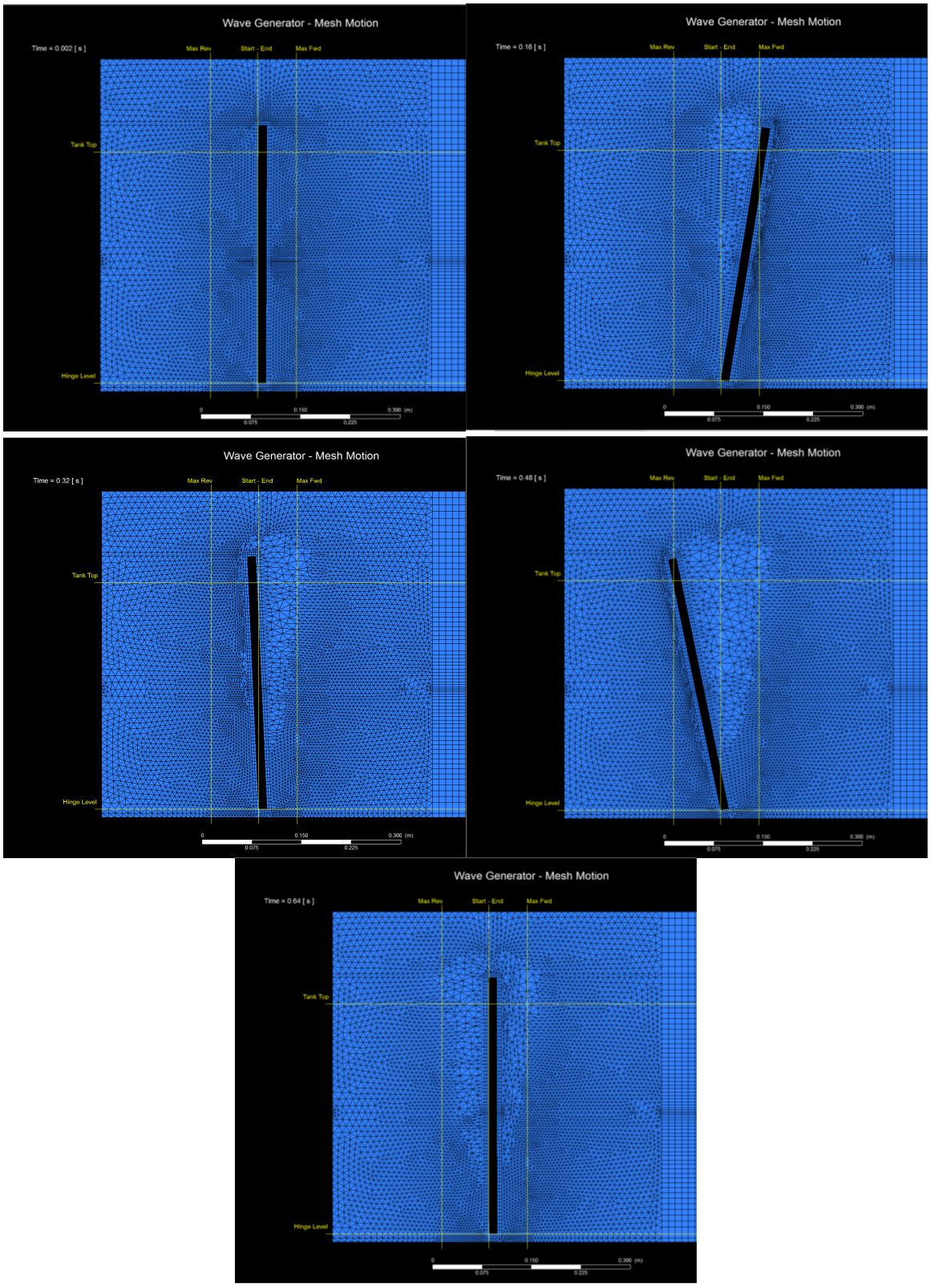

Figure 2.12 Wave Generator behavior and mesh condition at t=0, ¼, ½, ¾ and 1 cycle into the simulation

2.3.2 Torque Observations

Examining the Torque versus Time over 40 seconds is a good starting point. Figure 2.13 shows a comparison of the experimental data, and the Fixed Wing and Moving Wing models. The data was a measure of the torque generated about fixed point at the leading edge of the Wing. To compare appropriately, the time series for each data set has been shifted to align with the others as closely as possible.

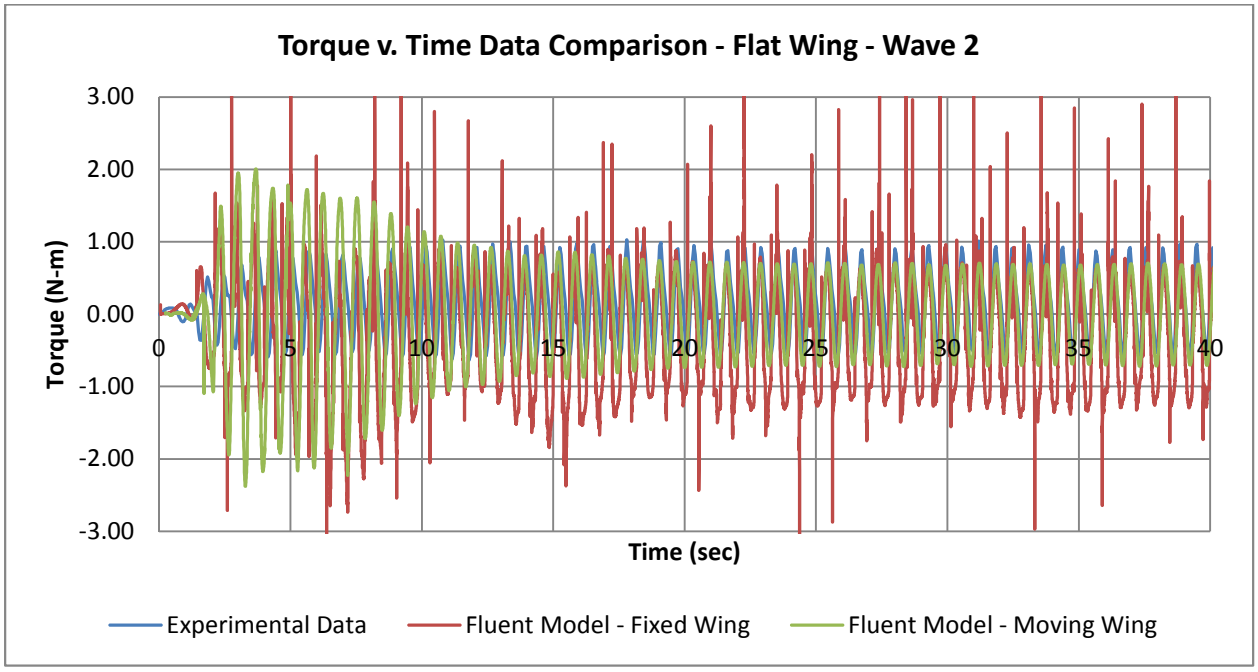

Figure 2.13 Torque data comparison. 0-40 seconds

Looking at the overall torque versus time graph over the entire simulation makes it difficult to really interpret what is happening, however it does allow for a couple observations. The Fixed wing model is clearly undergoing some events that show up as spikes in the data, and it also appears to have much higher negative torque peaks than both the measured data and the Moving Wing model. It is apparent that even though there are differences between them, all of the data sets achieve a level of equilibrium after only about 12-13 seconds. For additional comparisons it will be assumed that at 20 seconds all models and the experimental data have reached an equilibrium point.

Figure 2.14 shows the same Torque versus Time graph, but truncated to the portion of the graph where both the models and the experimental data have reached equilibrium.

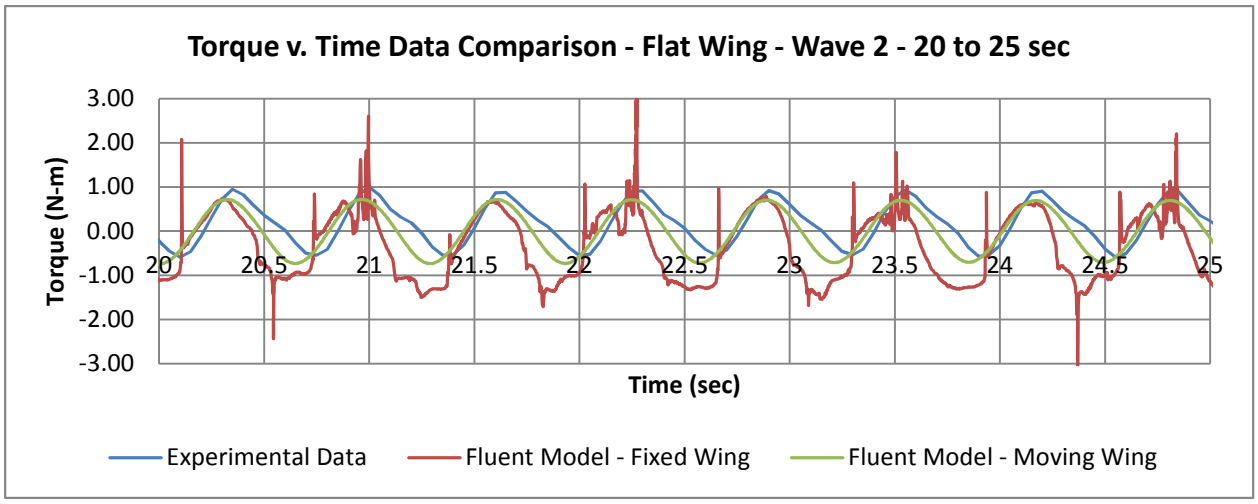

Figure 2.14 Torque data comparison. 20-25 seconds

From this data, it's clear that the frequency between both models and the experimental data is very close; which reinforces the point that the Wave Generator is functioning appropriately. An observation about the experimental data can be made here. The data was taken with a sampling rate of 20 Hertz, which appears to capture the torque maximums and minimums, however there are some clear points in the data, and it could definitely improve from a higher sampling rate.

Looking at the fixed model torque data, the frequency is clearly there but there are several oddities with the data. The first are the large spikes found occasionally at both the maximum and minimum torque spikes. These can be attributed to the unforgiving constraint of the Wing being fixed in place. With the Wing fixed, there is no transfer of energy through the Wing, so when a wave impacts the bottom of the Wing, it creates a large spike in torque. Additionally there appears to be steep transitions between the maximum and the minimum torque values. Examining the Moving Wing data, it shows better agreement with the

experimental data, however the curve of the experimental data has more of a triangular shape than that of the Moving Wing data.

2.3.3 Volume Fraction Observations

Examining the fluid motion itself sheds its own peculiarities. Figure 2.15 shows several images captured during the execution of the test, while Figure 2.16 shows both the Fixed Wing and Moving Wing models fluid behavior at a similar timestep.

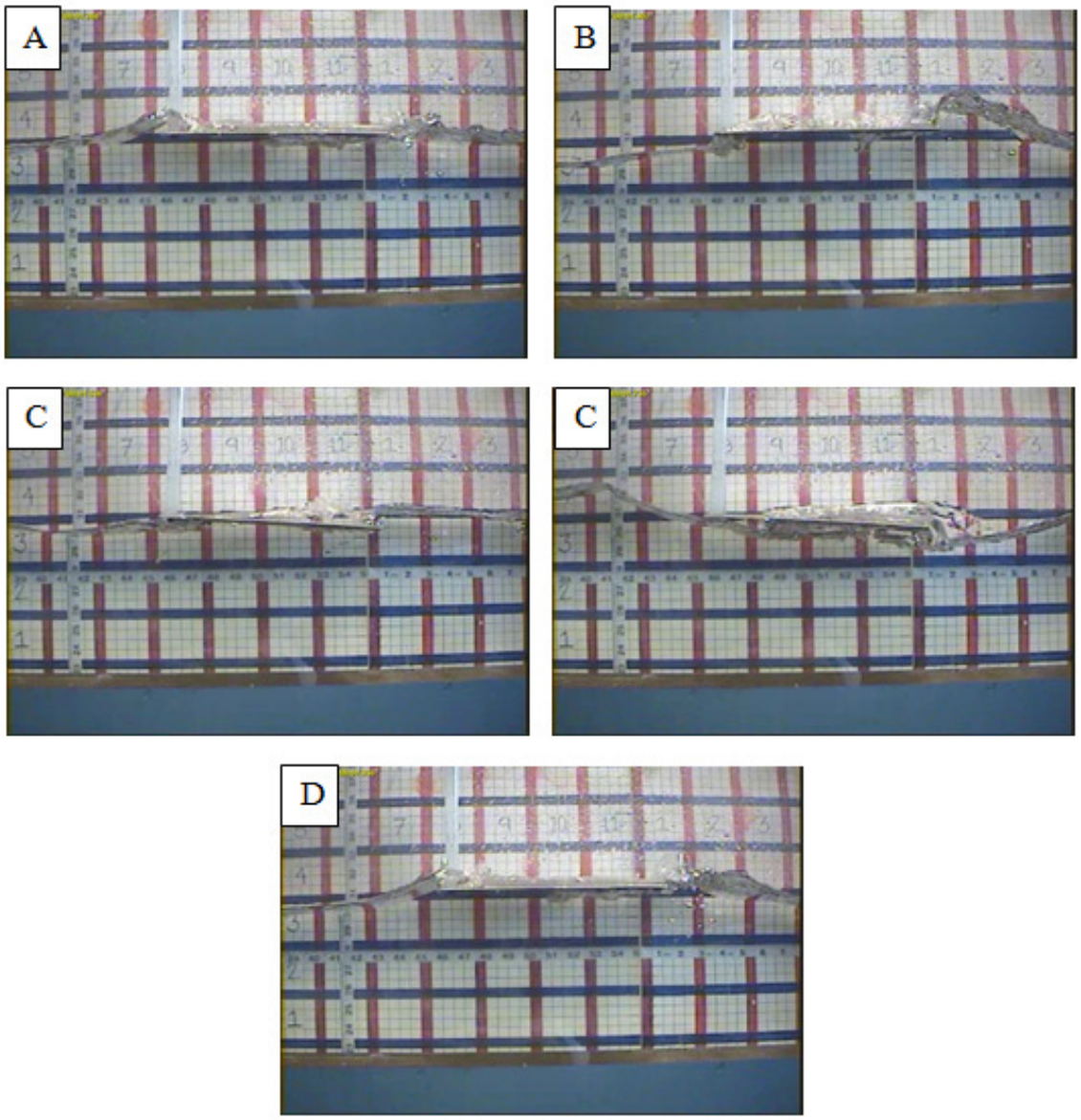

Figure 2.15 Images of the fluid behavior during an experiment with the Wing in the WMU wave tank. (*Durren, 2012*)

There are several observations that can be made here as well. The fixed Wing model produces waves that are larger and much more like the waves that are found in the actual wave tank experiments. There is entrainment of air in the water with the Fixed Wing, whereas with the Moving Wing model there is none to be seen. By comparison the Moving Wing model waves appear to die out as they progress down the tank. This is consistent with some behavior seen when the CFX program was used as well, and can be traced to the Compressive VoF

scheme. Lastly, the surface of the Fixed Wing model appears much more clear and defined than that of the Moving Wing model. This is to be expected as well, due to the usage of the geo-reconstruct volume fraction scheme.

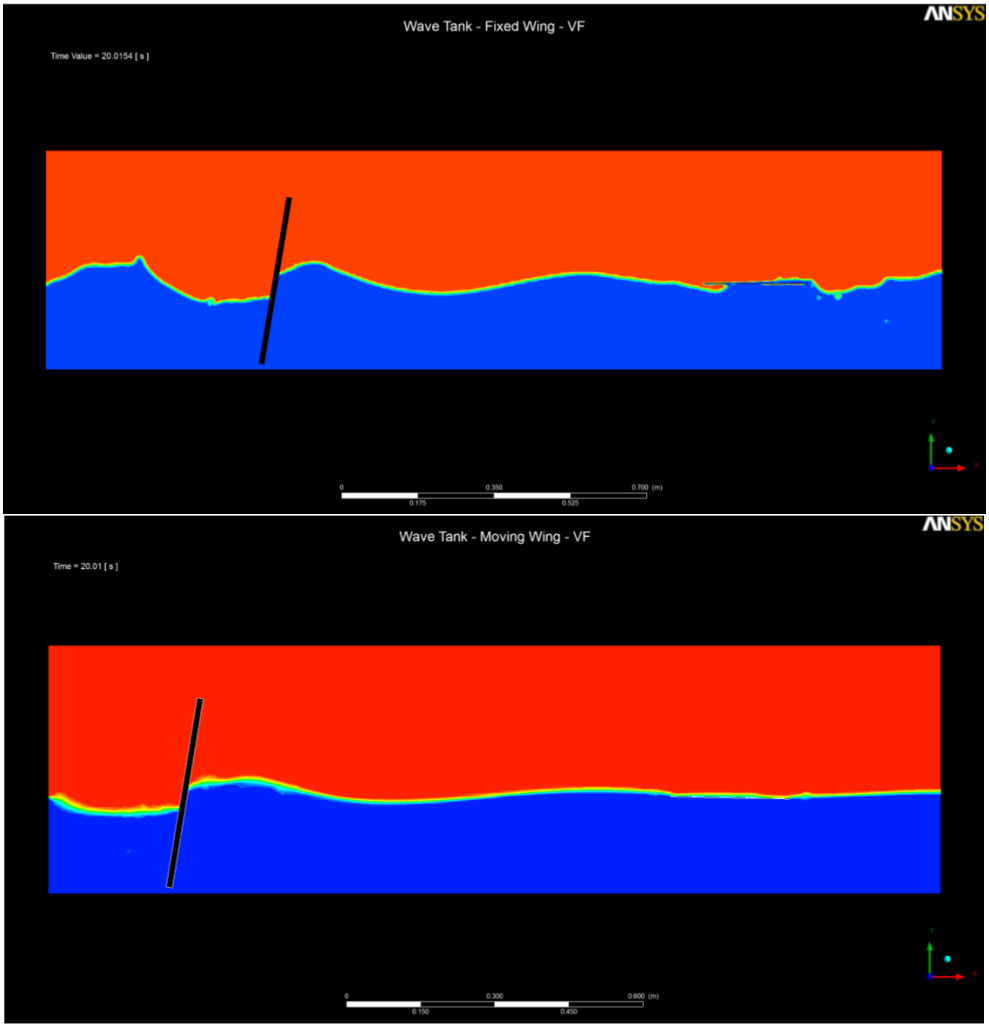

Figure 2.16 Comparison of fluid motion at t=20 seconds of the Fixed Wing model (top) and Moving Wing model (bottom)

2.3.4 Fixed Wing Anomalies

Regardless of the fluid behavior of the Moving Wing model, the torque values match very well to the experimental data, therefore focus can be put on understanding the behavior of the Fixed Wing model. There are several anomalies in the torque data that need to be

addressed. Figure 2.17 shows the torque values from 20 to 21 seconds. In this time range the data spikes and torque ramps can be more clearly seen.

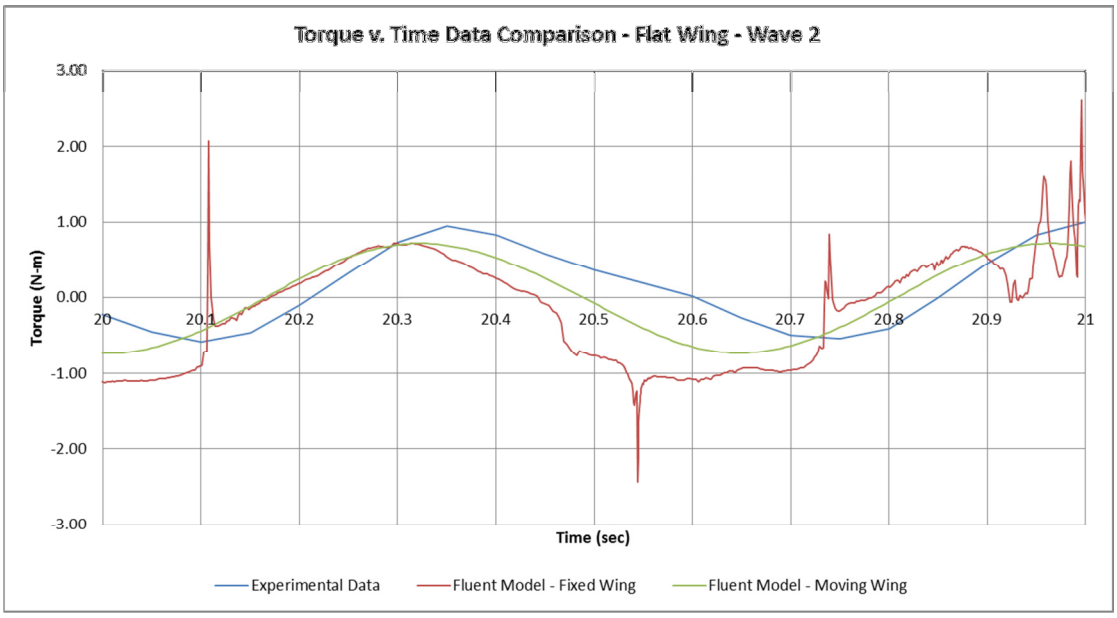

Figure 2.17 Torque data comparison. 20-21 seconds

To explain these torque fluctuations, a closer look at the fluid behavior is required as well. Figure 2.18 shows a closeup of the fluid motion around the Wing for both models at t=20 seconds. There is clearly a difference between the two models at this point. The Fixed Wing model shows both the previously mentioned entrainment of the air in the water, as well as the larger surface waves. This can help explain the torque spikes as well. The large torque spikes can be traced to waves impacting the surface of the Wing. In the Moving Wing model, this causes the Wing to move slightly, however in the Fixed Wing case the Wing cannot move, and thus absorbs much more energy, which shows up in the torque data as a spike. The large ramps can also be explained by this same limitation. Because the Wing is fixed in place, with air trapped underneath, it has no buoyancy force pressing up from underneath, thus causing a torque drop. A similar instance would be seen when the water level would put pressure on the bottom of the Wing.

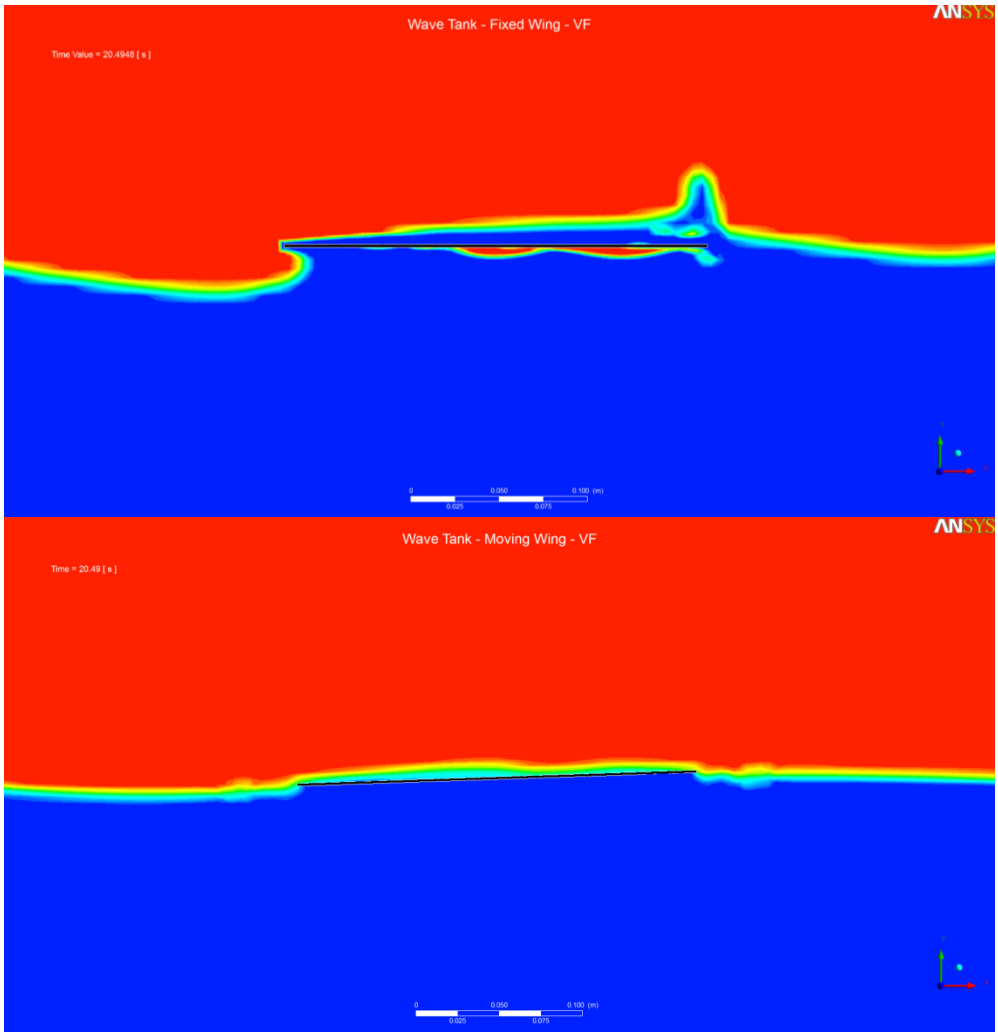

Figure 2.18 Comparison of the fluid flow around the Wing at t=20 seconds for the Fixed Wing (top) and Moving Wing (bottom) models

Both of these situations are caused by the boundary conditions which constrain the Wing from moving. Removing those constraints by allowing the Wing to move should improve the data set.

2.4 Wave Tank Conclusions

There are several important conclusions that can be drawn from the CFD models. The first is that depending on what the intent of the model is, the setup of your model could be very different yet accomplish the same goal. The model that better recreated the waves in the tank was the Fixed Wing model. This is due to the fact that the volume fraction scheme used was the more accurate geo-reconstruct scheme. It's worth repeating though that this scheme required the usage of variable timestepping to stay stable, and required much longer to run than the Moving Wing model.

However if the goal of the model is to accurately recreate the torques felt by the Wing, the Moving Wing model did a better job of this. While the Fixed Wing model was close in general shape there are many torque spikes that do not occur in the wave tank due to the Wing not being fixed.

It is also worth noting that these simulations were run for up to 60 seconds in length, to ensure they have reached an equilibrium point. Upon analyzing the results, it is clear that only 15-20 seconds is required to reach equilibrium, at which point it would only need to be run for several more seconds to obtain valuable data. This would drastically shorten the amount of time needed to run, however are must be taken in any subsequent simulation that the equilibrium has been reached, and that the simulation was not shutdown too soon.

Ultimately, the preferred model in this case is the Moving Wing model, as it does a job god of replicating the wave motion, and accurately recreates the torques as well.

2.5 Wave Tank Recommendations

In general, the Fixed Wing model should not be used. The Moving Wing model did a better job of replicating the torques seen and provided a more stable, faster solving model than

its Fixed Wing counterpart. However depending on how critical the flow is, the Moving Wing model should be modified to use the geo-reconstruct volume fraction scheme. This should provide more accurate wave motion and still contain the accurate torque data. However to do this the mesh around the Wing must be refined, variable timestepping will be required, and the under-relaxation factors adjusted, which will all increase the solver time.

Finally, if further experiments are conducted with the wave tank, the sampling rate of the strain data in the wave tank should be increased. When focusing on the finer aspects of the torque data, it can be clearly seen that there could be missed torque spikes in the data.

3 SEA WALL – 3D MODEL

3.1 Problem Introduction

After examining the wave tank problem closely, it was discussed whether further development of the model was necessary or if an investigation into other means of energy absorption from waves would be more beneficial. The latter was decided upon and an investigation was started into attempting to absorb energy from waves via vertical plates instead. The goal of the project was to develop a model replicating waves of a similar size as to those in the wave tank model, impacting a wall similar to a sea wall. Sea walls cover much of the shoreline of oceans, lakes and rivers. Determining if the energy fluctuations found in small waves could be harnessed is intriguing.

Additionally it was required that this model be able to examine waves impacting the wall at an angle, and waves of different wavelengths, therefore three separate runs with the same underlying parameters will need to be run. As this project was closer to an examination of how waves interact with a vertical surface, reflections from the boundaries needed to be limited.

3.2 Model Simulation & Setup

3.2.1 Problem Discussion & Goals

Just as in the 2D model, there are several important characteristics that must be addressed prior to putting the model together. The first is the actual geometry of the sea wall that the waves will be impacted against. Because of the requirement that the model be capable of generating waves with numerous impact angles, and not simply perpendicular, the model must become three dimensional. This carries numerous additional concerns that will be covered, but most of all the number of nodes in the mesh will increase dramatically, causing the

simulation to take longer to run. Therefore care must be taken to optimize the mesh well and to limit the capabilities of the model to specifically what it was tasked for.

As a point of comparison between the models, the force on the Sea Wall will be measured directly, and the source of this force needs to be identified.

Additionally the focus of the model will be on extracting energy from a few travelling waves, not the standing waves as was done in the 2D models previously. Also there should be limited reflections as the idea is to determine how much energy is extracted from the waves themselves, not including reflections from the boundaries or other sources. This has several effects on the design of the model. Most importantly the model will have a short simulation time, because reflections from the boundaries will occur if the model runs for too long. The idea then is to generate 2-3 waves, have them impact the wall, and then dissipate quickly before reaching the boundaries of the model.

With these points of focus in mind, three models were conceived for comparison.

- Model 1 - Baseline: Use same wave characteristics as in 2D model (amplitude cut in half)
- Model 2 - 15 Degree: Same as baseline, with 15 degree impact angle
- Model 3 - Long Wavelength: Uses a longer wavelength wave

The following wave characteristics were determined for each model as well.

Table 3.1 Comparison of the waves parameters for each of the models

Model #	Frequency (Hz)	Amplitude (m)	Wavelength (m)	Heading angle (deg)	# of Waves Generated
1	1.56	0.022	0.612	0	3
2	1.56	0.022	0.612	15	3
3	0.97	0.0125	1.223	0	2

3.2.2 Problem Setup

3.2.2.1 Wave Generator

The Inlet, or Wave Generator, was simple a velocity inlet that made use of the open channel wave boundary function in Fluent. This function works similarly to the open channel function, in that the height of the water is set, but it also allows for the generation of waves by providing the amplitude, wavelength, phase, wave heading direction and the type of wave being generated. This function is convenient for this project because changing the wave direction is as simple as changing the heading option. This simplified the model as well, as no moving walls or meshes are required either.

3.2.2.2 Geometry and Design

Figure 3.1 depicts the final geometries of the model. Essentially the sea wall is located in the center (red), surrounded by (outlets), and the previously described inlet (green) designated the Wave Generator. Having determined that the open channel wave boundary condition would be used, this had several effects on the design of the model. First the entire mesh could be generated via an H-grid. With the boxy shape and sharp corners this makes meshing easier, and it will reduce the computational time. Also because the open channel

boundary condition cannot handle reflected waves interacting with the waves being generated, the wave generator can only generate waves as long as that does not occur.

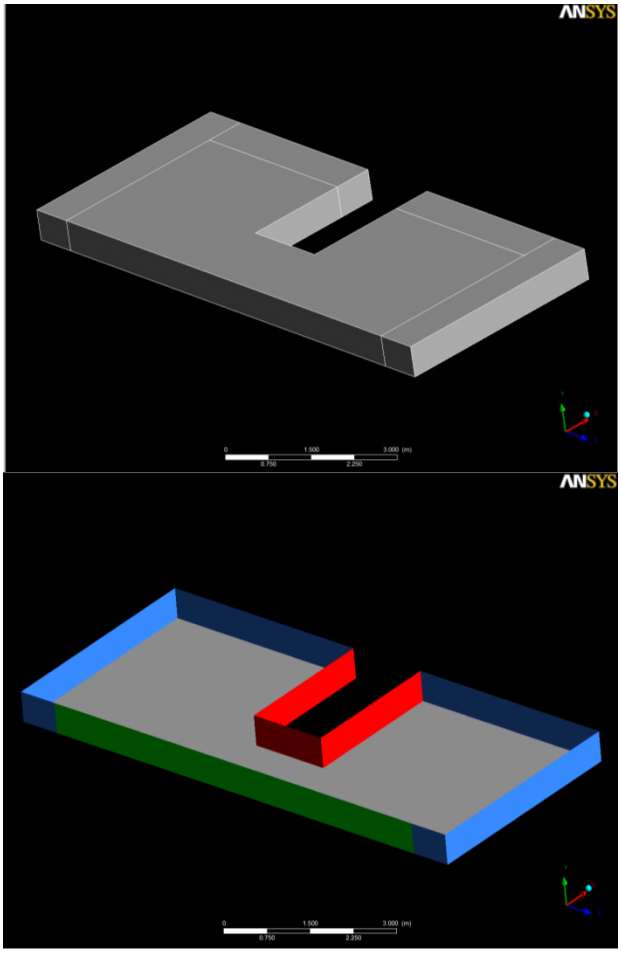

Figure 3.1 Geometry and Boundaries for the three models. Sea Wall (red), Outlets (blue), and Wave Generator (green)

It was necessary to limit reflections from the boundaries of the model as well. As is seen in Figure 3.1, the model is broken up into 5 regions. The large middle region including the Sea Wall Front, is the main fluid region. The other 4 regions all employ a numerical beach that will be discussed later. This beach dampens out the waves as they pass into the region, diminishing most of the wave energy. Additionally the distance between the boundaries and the Sea Wall Front was optimized to minimize the size of the model, which would allow for faster

computational time, but be large enough that the boundaries would not affect the results. However if someone were to run a simulation for rather extreme wave angles, the boundaries may need to be extended.

3.2.3 Boundary Conditions

All of the Sea Walls and the Bottom use the wall boundary condition. Friction was ignored and wall adhesion was left off. These could easily be enabled if so desired, however for the purposes here they would only increase the computational time. The Top of the model is entirely a pressure outlet, with the pressure being set to zero gauge pressure.

There are four outlets in this model, and all of them are setup with the same boundary conditions. They are all pressure outlets that make use of the open channel boundary function, similar to the Front in the previous wave tank model. There is a danger with using this function however, and it involves wave reflections. Because the open channel boundary condition has a fixed fluid surface level, when a wave approaches, the trough of the wave will drop below the fixed surface height of the boundary. This will cause a wave to propagate away from the outlet, which could interfere with incoming waves. In the previous model wave reflections from the boundary were largely ignored, due to the fact that the reflections were on the backside of the Wave Generator, and didn't have any impact on the parts of the model we were interested in, that being the Wing. However, in this case the reflections could interfere with oncoming waves that are impacting the Sea Wall, therefore the waves must be damped out. Therefore, the outlets make use of another function called the numerical beach. The numerical beach function allows for damping of incoming waves, which can reduce or completely eliminate reflections. The direction of the damping and the scale of the damping can be set within the functions options. For this simulation, the four outlets each have a separate numerical beach that acts on

waves travelling perpendicular to the outlet. This was found to work very well for eliminating the reflections completely.

3.2.4 Mesh

Figure 3.2 shows the mesh developed for the model. It consists entirely of hexahedral elements and was designed to have a very fine mesh near the sea wall and at the corners. The mesh gets courser as the distance from the wall increases. Also from the front and side views, it can be seen that the mesh around the water's surface is denser.

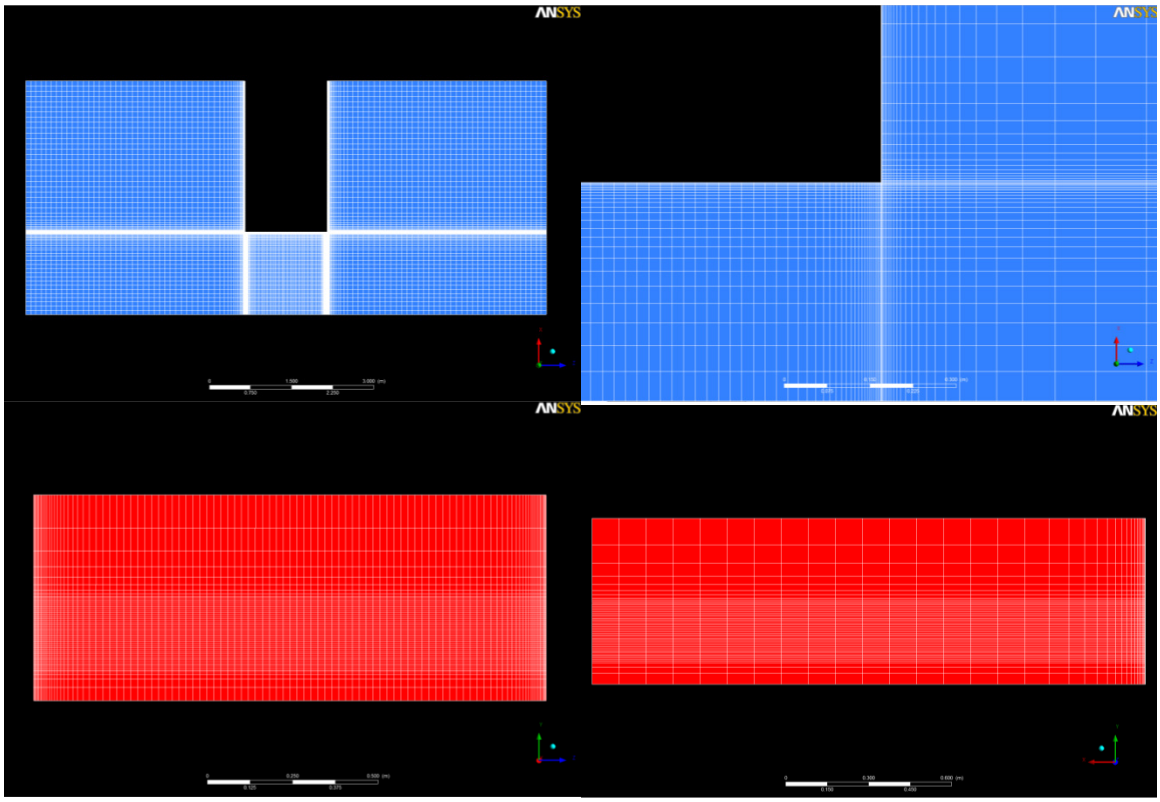

Figure 3.2 Severeal views of the mesh. Overall top (upper left), Right corner (upper right), Sea Wall Front (lower left), and Sea Wall Side (lower right).

3.2.5 Material, Phases & Operating Conditions

These parameters were all setup identically to the wave tank model described above, with one exception being the reference pressure location. However the idea for the placement of the reference pressure location is the same, as it was placed very close to the Top boundary, and in a location that would constantly be at zero gauge pressure.

3.2.6 Solution Initialization & Solver Settings

The following is a breakdown of all the solver settings used in the model. The Fluent documentation provides very good descriptions and usage criteria and therefore it is unnecessary to be repeated here.

Table 3.2 Solver Models used in the Sea Wall Project

Models	
Multiphase Model	Turbulence
Volume of Fluid - Explicit	SST k-ω

Table 3.3 Solver Schemes used in the Sea Wall Project

Schemes						
Pressure-Velocity Coupling	Gradient	Pressure	Momentum	Volume Fraction	Turbulent Kinetic Energy	Turbulent Dissipation Rate
PISO	Least Squares Cell Based	PRESTO!	Second Order Upwind	Compressive	Second Order Upwind	Second Order Upwind

The following is a list of the under-relaxation values used in the models.

Table 3.4 Under-Relaxation factors used in the Sea Wall Project

Under-Relaxation Factors						
Pressure	Density	Body Forces	Momentum	Turbulent Kinetic Energy	Specific Dissipation Rate	Turbulent Viscosity
0.5	0.5	0.5	0.5	0.5	0.5	0.5

The model was initialized in the same way as the wave tank model, with exactly the same water depth. Upon initialization, Fluent automatically calculates and applies the hydrostatic pressure expected.

For this project the simulation was executed in three steps. In this case it wasn't to improve the stability of the model, but to stop the wave generator after the desired number of waves had been generated. As discussed, the Wave Generator functions by using the open channel wave boundary condition, which does not properly handle the interaction of reflected waves. Therefore to analyze how the waves dissipate, the wave generator must be shut off, and the reflected waves absorbed in a similar manner as the outlets. In this case after the three waves were generated, the simulation was halted and the boundary condition was then changed to a pressure outlet, utilizing the open channel boundary function. However before enabling the numerical beach the simulation was restarted for a short amount of time, to allow the wave that was just completed, to clear the region to be assigned the numerical beach. After this region had been cleared, the simulation was stopped again, and the beach enabled. Also, as stated in the problem statement, three separate runs were conducted to examine how wave heading angle and wave frequency and amplitude impact the flow around the Sea Wall. Because Model 3 had longer a longer wavelength but used the same geometry it required slightly different timing, as only two waves could be generated. Therefore table 3.5 lists the timings used for Models 1 and 2, and table 3.6 lists the timings used for Model 3.

Table 3.5 Time information for Models 1 & 2

	Timestep Size (s)	No. of Timesteps	Total Time (s)
Part 1	0.002	960	1.92
Part 2	0.002	375	0.75
Part 3	0.002	1165	2.33
Total			5.0

Table 3.6 Time information for Model 3

	Timestep Size (s)	No. of Timesteps	Total Time (s)
Part 1	0.002	1010	2.02
Part 2	0.002	100	0.20
Part 3	0.002	1390	2.78
Total			5.0

3.3 Sea Wall Results

3.3.1 Validation

Before examining the results in detail, it was first necessary to examine the validity of the model. Unlike the wave tank project, there is no data to compare against. Therefore other means of validation are required, starting with a calculation of the initial force imparted on the wall. Initially there is no movement of the water, and all the force being put on the Sea Wall Front will be due to the weight of the water itself, which is simply the hydrostatic pressure. Appendix A demonstrates this calculation, which provides a value of 279.265 N. Figure 3.3 shows the force on the Sea Wall Front versus time, and it is clear that at $t = 0\ s$, that force is very close to the anticipated value.

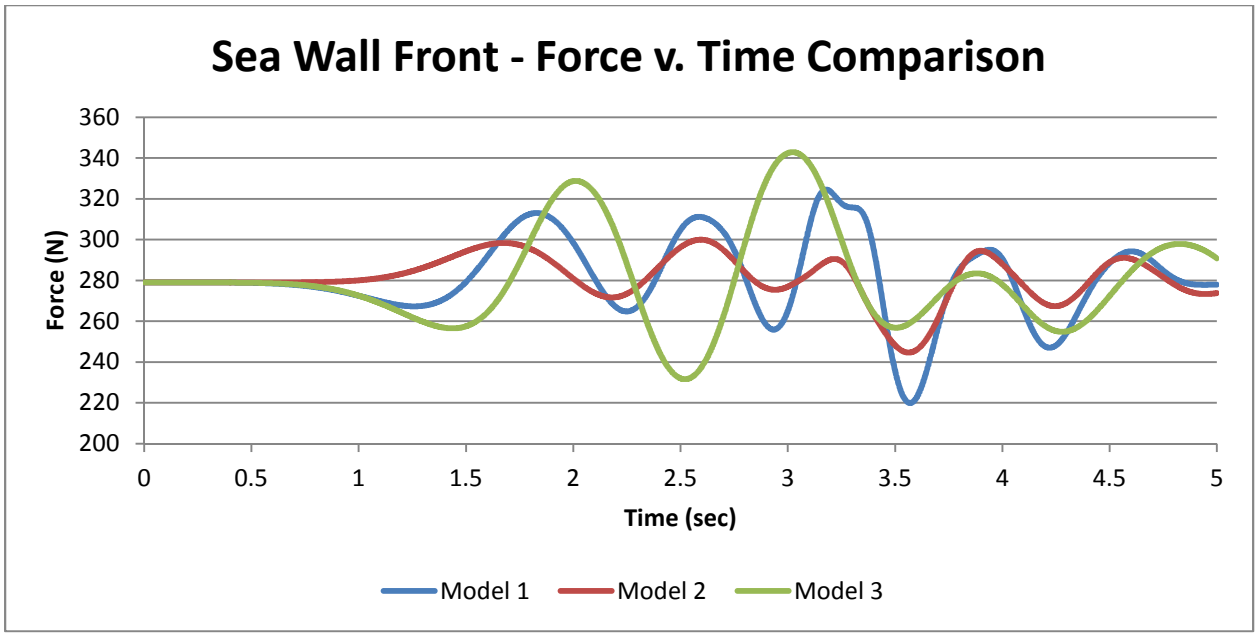

Figure 3.3 Comparison of Force on the Sea Wall v. Time for each Model.

A further observation that can be used to validate the models is that of the period of the waves being generated. It is expected that the relationship between the force on the wall and the height of the water should be very close, and therefore as was just described previously, the force on the wall will be directly related to the amount of water against it. Therefore the period of minimums and maximums on the force graph should be very close to the period of the waves being generated. This proves to be true as well.

Having made the previous observations from Figure 3.3, its expected then that when the water surface is rendered, that the motion of the waves should be quite smooth, with very little or no splash present. Figure 3.4 shows the surface of the water at several timesteps from Model #1, and this is exactly what is seen. The same observation can be made of the other models as well.

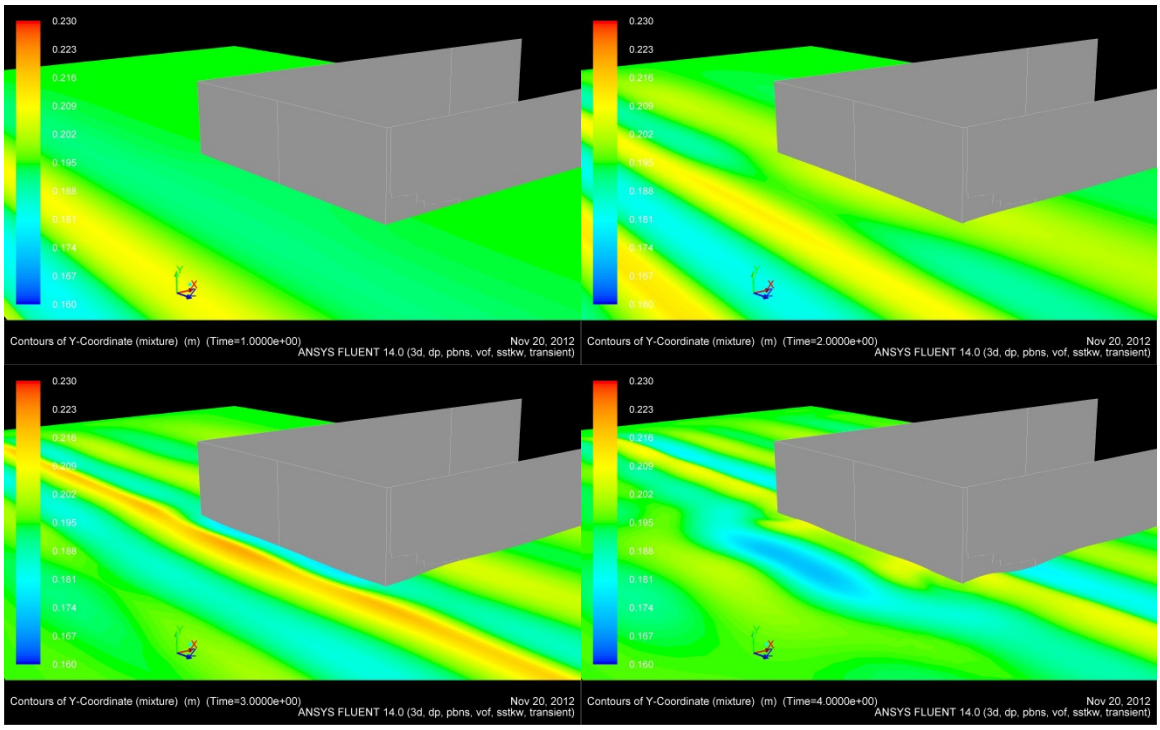

Figure 3.4 Model #1 Fluid Flow at t = 1, 2, 3, and 4 seconds

Key to the model was the inclusion of the numerical beach, and verifying that it is performing as desired is also critical. The intention was for the waves to be completely dampened out before they reached the boundaries of the model. This would prevent wave reflections from these surfaces from interfering with the forces being generated on all surfaces of the Sea Wall. In Figure 3.4 observing the far boundary, it can be seen that the water surface is calm at all timesteps near the wall. The same behavior is present in Model #2 and #3, and along the other boundaries.

From these initial observations and calculations, the models presented were considered to be valid for the purposes of which it was designed. However several oddities were observed as well.

3.3.2 Wave Phenomena

Accepting that these models are not fatally flawed, a closer look can be made at the force on the Sea Wall Front. Referring again to figure 3.3, attention needs to be paid to Model #1 and

the force between 3 seconds and 3.5 seconds. There is an extended force peak during this time frame that is unexpected. Figure 3.5 shows the water's surface rendered during this timeframe.

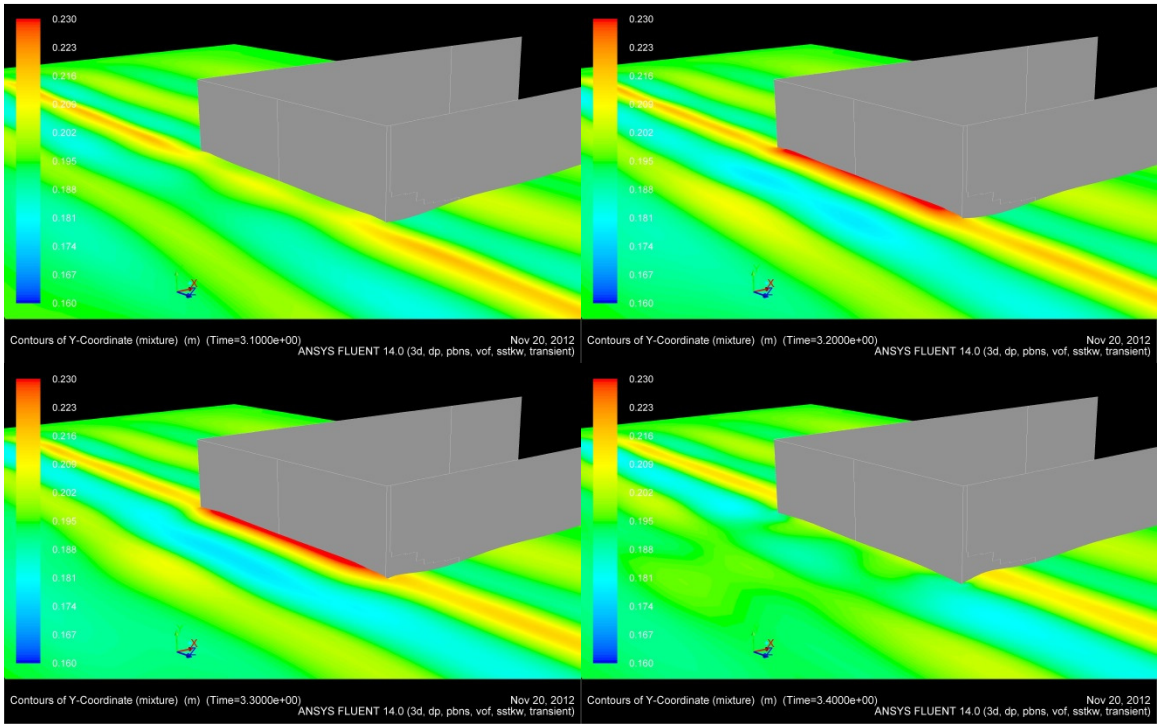

Figure 3.5 Model #1 Fluid Flow at t = 3.1, 3.2, 3.3, and 3.4 seconds

What was noticeable is the myriad of wave heights, both along the Sea Wall Front, and on the surface of the water in general. At first this was unexpected, as the waves being generated were perpendicular to the Sea Wall Front, any reflection should also be directed perpendicular to the wall.

In an effort to understand what was causing the varied wave heights and the strange force on the Sea Wall Front, the water height was more closely examined very near to the wall. Using CFD-Post, several lines were drawn along the Sea Wall Front, and the pressure along these lines plotted versus time and location(Figure 3.6). These plots show how the force on the Sea Wall Front has varied in different locations across the face of the Sea Wall Front. What can be noted from these plots is that they again show the varying heights associated with the depth of the water. What is also interesting is what is happening at the corners. There is a sharp upward

trend in force at each corner that descends through all the plot levels. This indicates something could have been occurring at these corners, and a closer look is necessary.

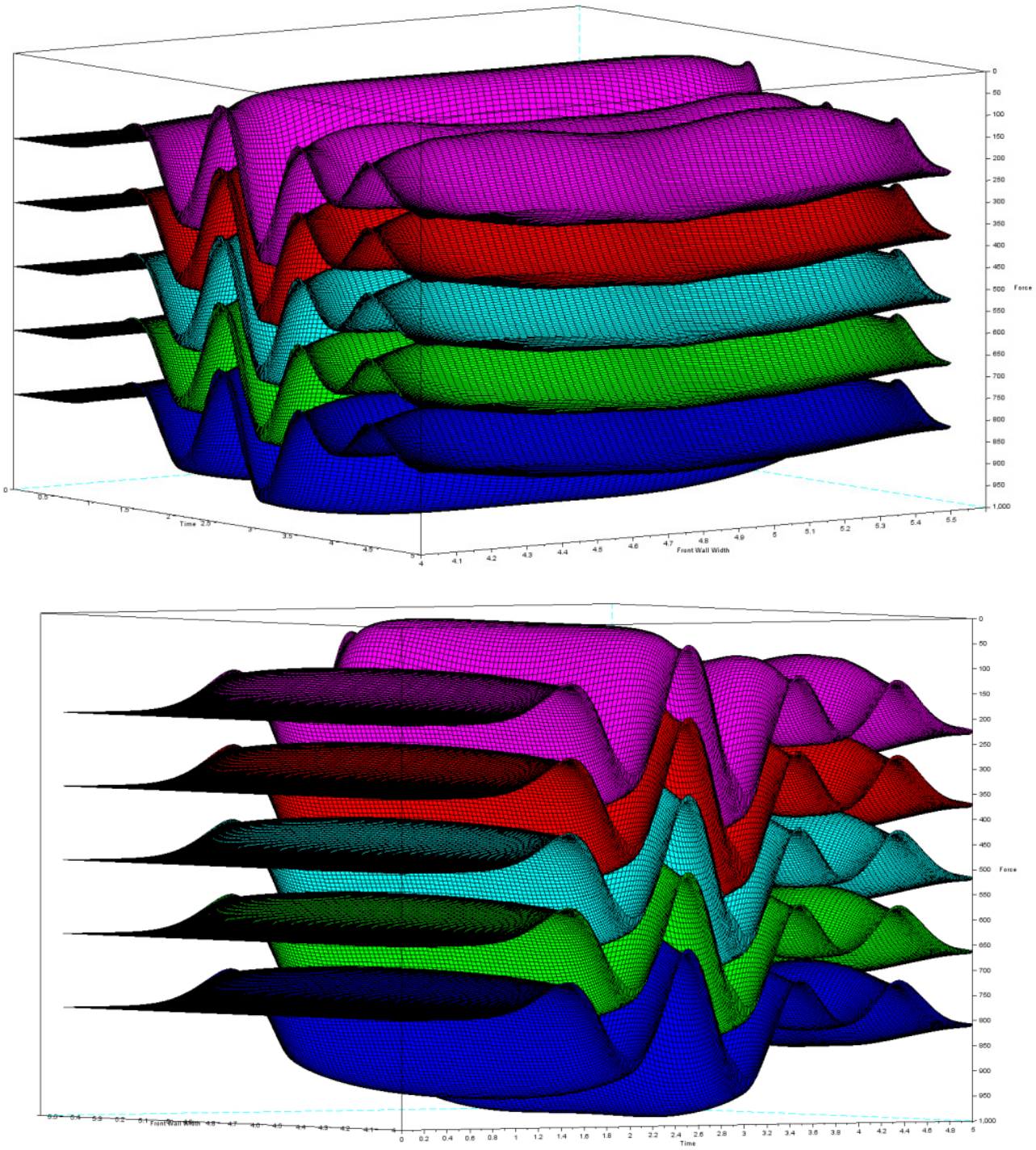

Figure 3.6 Plots of Force v. Time v. Location on the Sea Wall Front at five different depths

Focusing closer on the corners, and again using CFD-Post, a plane was drawn parallel to the Sea Wall Front, but set 1.0 millimeter from surface. Plotted on this surface are the velocity vectors of both fluids projected onto the plane. A line was plotted as well, which defines the water's surface. The idea behind this plane was to both confirm the various wave heights along the Sea Wall Front, as well as determine the flow direction of the water near the Sea Wall Front at the corners. Figure 3.7 contains several frames from this animation.

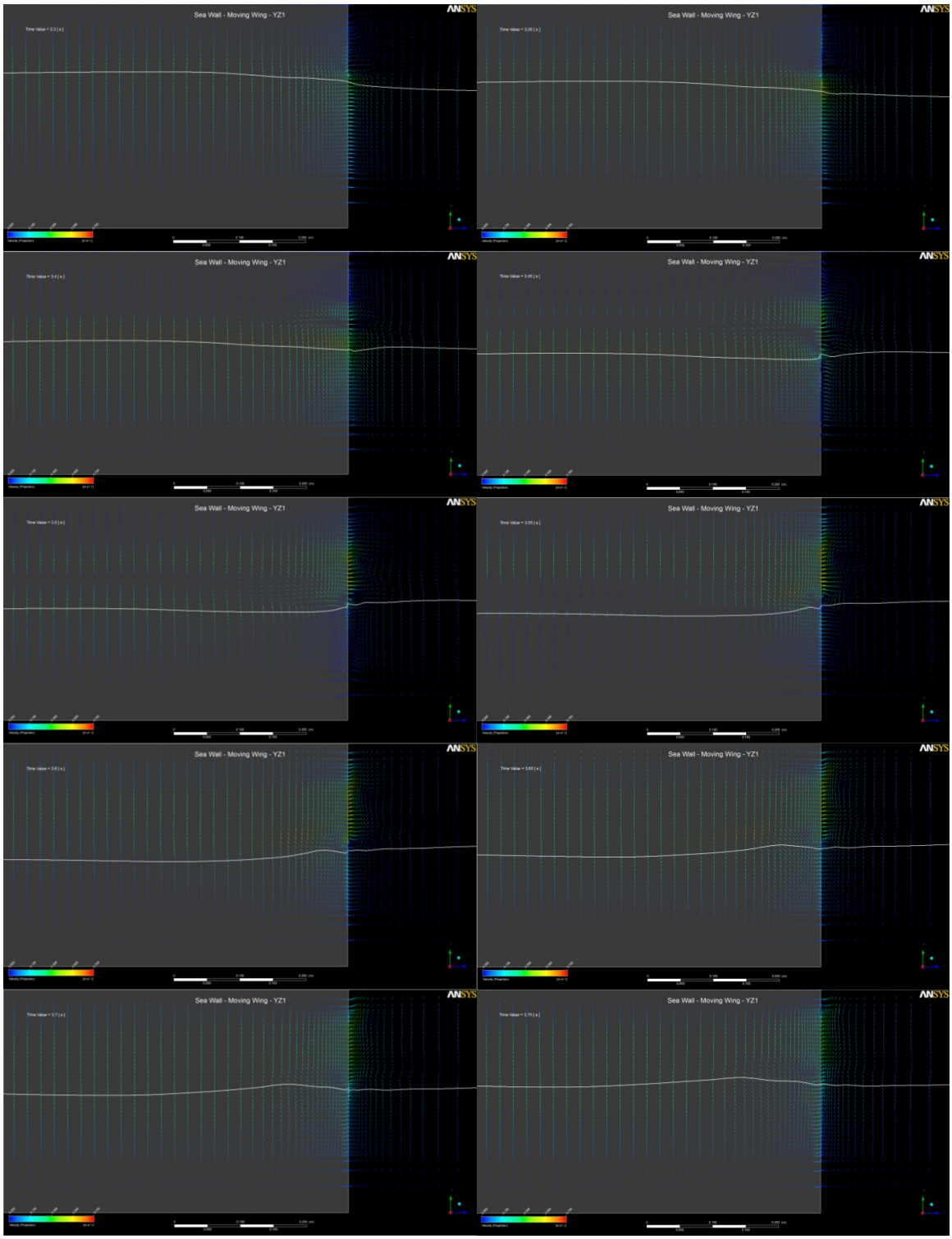

Figure 3.7 Velcoity Vectors plotted on a plane set 1 mm from the Sea Wall Front, for times between 3.3 and 3.75 seconds

Several conclusions can be drawn from this animation. First, the various wave heights can be confirmed along the Sea Wall Front, as is evident by the water surface line. Second, the boundary condition that was intended to absorb all incoming waves and prevent reflections is working properly, and therefore the varying heights could not be caused by waves incurred by reflections from the boundaries. Most importantly, it appears the corners of the Sea Wall Front may be the source of this phenomenon. Evidence for this appears to be as the water level drops after a wave has peaked, a wave begins to travel parallel to the wall away from the corner, along the Sea Wall Front, and it definitely appears to originate at the corner.

Continuing to focus on the corner, two animations were generated. The first depicted the velocity vectors along the water's surface as it moves near the corner (Figure 3.8). Paying close attention to the velocity vectors again, this animation gives a good indication of what is occurring. At the corner, the velocity vectors form a circular motion, resembling a vortex. The location of this motion is relative to the direction the water is flowing at the corner. This motion can be seen in the second animation that was generated (Figure 3.9). In this animation, a vortex identification function within CFD-Post was used to confirm the presence of the vortices and model them appropriately.

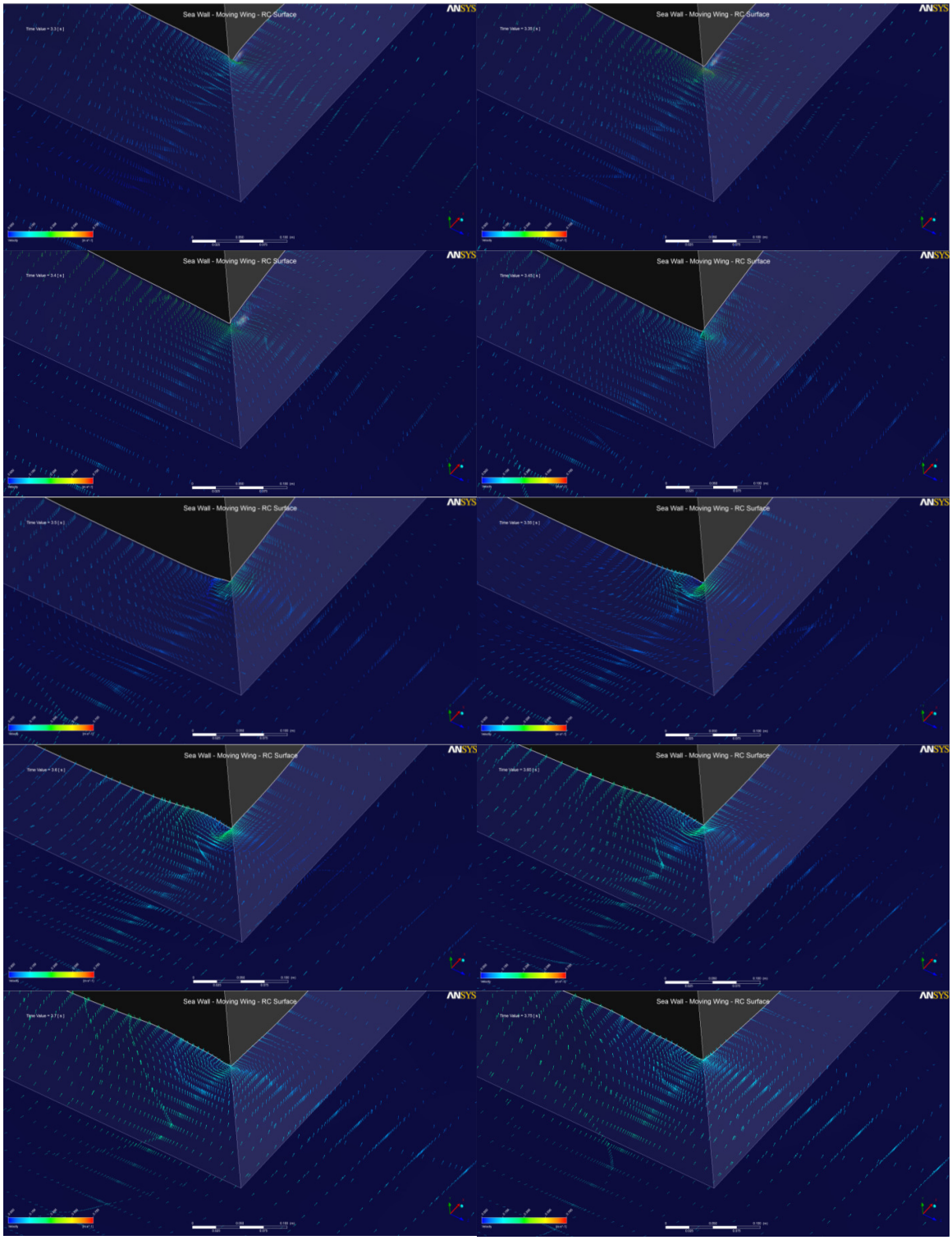

Figure 3.8 Velocity Vectors plotted on the water's surface near the right corner

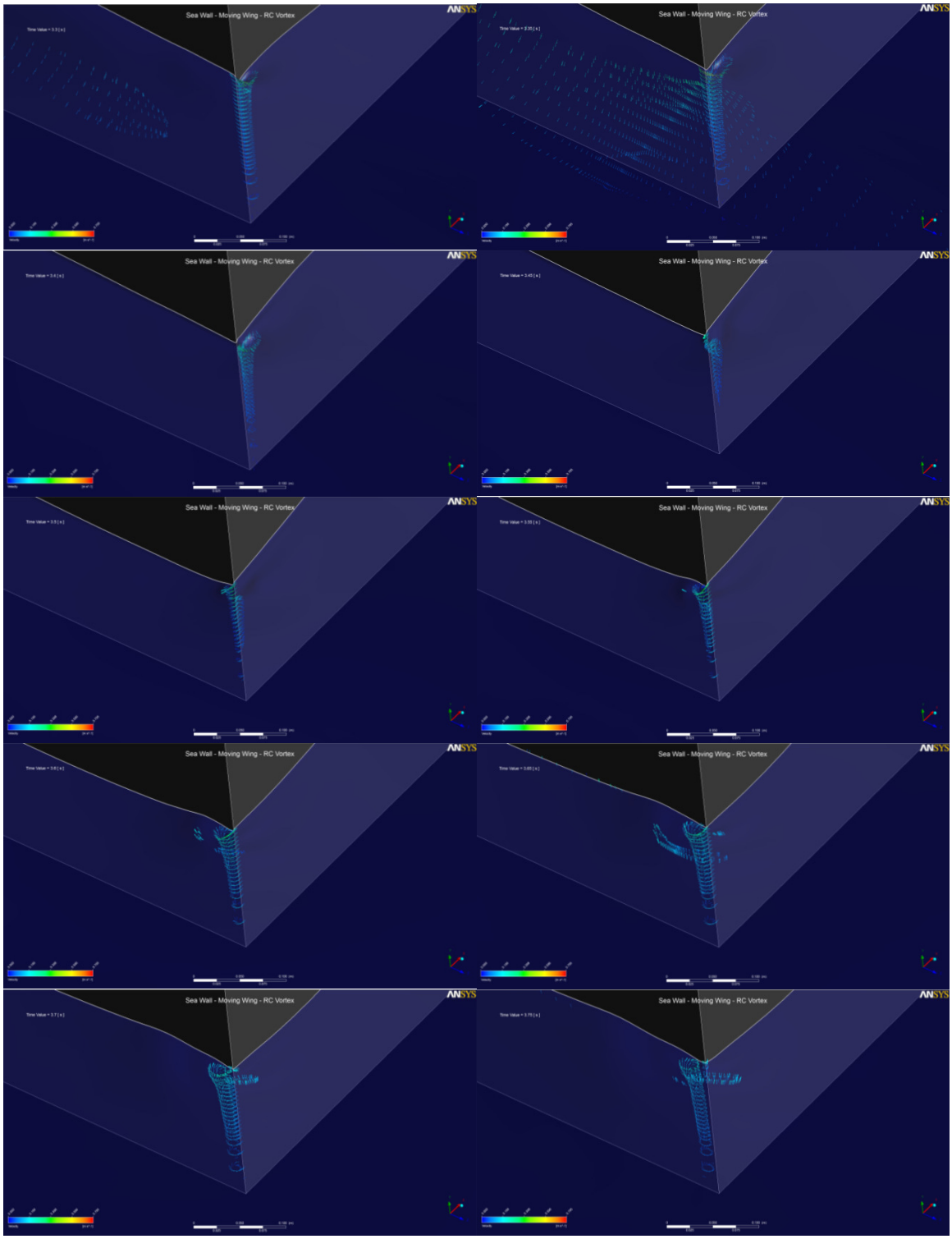

Figure 3.9 Velocity Vectors plotted on the vortex found near the right corner

As a wave peak approaches the Sea Wall Front, the water is flowing past the corner, generating the vortex downstream from the wall. As the water level drops to a trough the flow of water changes direction and heads back upstream at the surface. As the water returns around the corner, this changes the location of the vortex placing it in front of the Sea Wall Front and also changes the direction of rotation as well. Examining the timeframe when the transition between the two vortex locations occurs, the velocity vectors and position of the water's surface indicate that a wave has been generated in the direction that the vortex is about to form. This wave propagates outwards in all directions, not just along the Sea Wall Front, and is what is generating the various wave heights and mode shapes within the waves, which in turn explains the forces acting on the Sea Wall Front. This behavior was seen at both corners in all three Models.

3.3.3 Sea Wall Force

It needs to be stated that the maximum change in force on the Sea Wall Front is a significant value. Examining the largest maximum to the lowest minimum, and compensating for the area of the Sea Wall Front, Sea Wall saw force oscillations as large as 76 N/m, from a wave with an amplitude of 2.2 cm. This is not an insignificant value, and in the right circumstances could most likely be used to move some form of energy conversion device.

3.4 Sea Wall Conclusions

Several conclusions can be drawn from the three models developed. All three models achieved their intended goals of recording the force on the Sea Wall Front for various angles and wave conditions. More importantly, what was found is something as simple as a sharp corner, can have profound impacts on wave behavior. Additionally, the energy fluctuations found to be imparted on the Sea Wall Front were found, and the values were not insignificant.

3.5 Sea Wall Recommendations

These models were very simple, and focused solely on flow at the corner and near the Sea Wall Front. However based on the results found here, it should be no question that further study of this concept should be done. Additionally, it would be beneficial to modify the models to allow for breaking waves, where more of the force is due to the kinetic energy within the wave, than simply the hydrostatic force of the water placing pressure on the Sea Wall.

REFERENCES

ANSYS® Academic Research, Release 14.0, Help System, CFX, ANSYS, Inc.

ANSYS® Academic Research, Release 14.0, Help System, FLUENT, ANSYS, Inc.

Dahleh, M. D., and W. T. Thomson. *Theory of vibration with applications*. 5. Upper Saddle River, NJ: Prentice-Hall, Inc., 1998. Print.

Dean, Robert George, and Robert A. Dalrymple. *Water Wave Mechanics For Engineers And Scientists*. World Scientific Pub Co Inc, 1991. Print.

Durren, Rachel. "Absorber Geometry Optimization for a New Wave Energy Convertor." MS thesis. Western Michigan University, 2012. Print.

SC/Tetra. Vers. 9. N.p.: Software Cradle Co., 2011. Program documentation.

APPENDIX A:
HYDROSTATIC PRESSURE

The hydrostatic pressure is represented by the following equation:

$$P = \rho g d$$

Where *P* is the pressure, *ρ* is the fluid density, *g* is gravity and *d* is the water depth.

The force on the wall then is simply

$$F = PA$$

Where *A* is the area of the Sea Wall Front up to the surface of the water. The dimensions can be seen below in the figure.

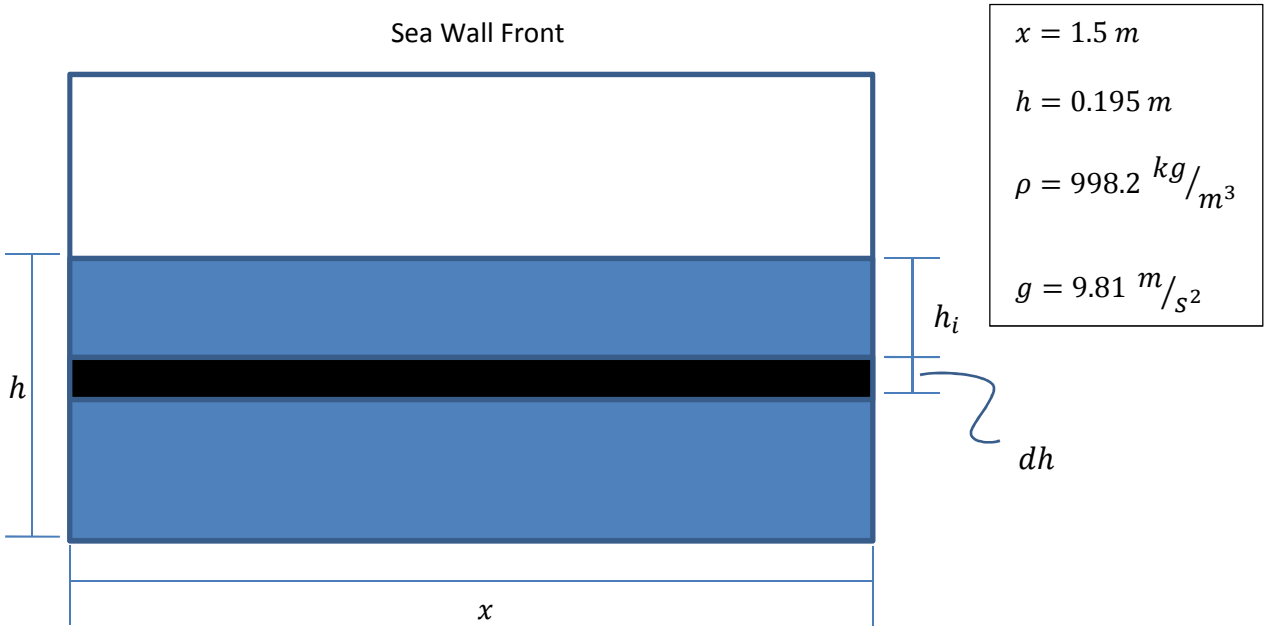

Since the pressure is constant for a specific depth, the equation for force on the Sea Wall only depends on the depth of the water. Therefore for rectangular area of depth h_i, the area dA becomes

$$dA = (x)(dh)$$

Combining the equations above, the force applied on the area dF, is

$$dF = PdA = (\rho g h_i)(x)dh$$

Integrating this over the water depth provides us with the force due to the hydrostatic pressure

$$F = \int_0^h dF = \int_0^{0.195} (998.2)(9.81)(1.5)h_i \, dh$$

$$F = 279.265 \, N$$

APPENDIX B:

2D – WAVE GENERATOR UDF

```
#include "udf.h"

real pi, freq, phase, w, AVel, A1, A2;

DEFINE_CG_MOTION(wallmotion, dt, vel, omega, time, dtime)
{
NV_S(vel, =, 0.0);
NV_S(omega, =, 0.0);

/* Defined Constants*/

pi = 3.141592654;
freq = 1.56;
A1 = .0478;
A2 = -.1790;
phase = -2.7836;

/*Define Wall Motion via. Angular Velocity */

w=2.0*pi*freq;                          /*angular freq in radians*/

AVel = -A1*w*sin(w*time + phase) + A2*w*cos(w*time + phase);

omega[2] = -AVel;                  /*Assign AVel to omegaz */
}
```

APPENDIX C:

2D – FLAT WING 6DOF UDF

```
#include "udf.h"

DEFINE_SDOF_PROPERTIES(Flat_Wing_6DOF, prop, dt, time, dtime)
{
   prop[SDOF_MASS] = .192;
   prop[SDOF_IXX]  = .032000;
   prop[SDOF_IYY]  = .033843;
   prop[SDOF_IZZ]  = .1;

   prop[SDOF_ZERO_TRANS_X] = TRUE;
   prop[SDOF_ZERO_TRANS_Y] = TRUE;

   printf ("\n2d_test_box: Updated 6DOF properties");
}
```

APPENDIX D:

WAVE TANK ANIMATIONS

Fluid Flow – Fixed Wing

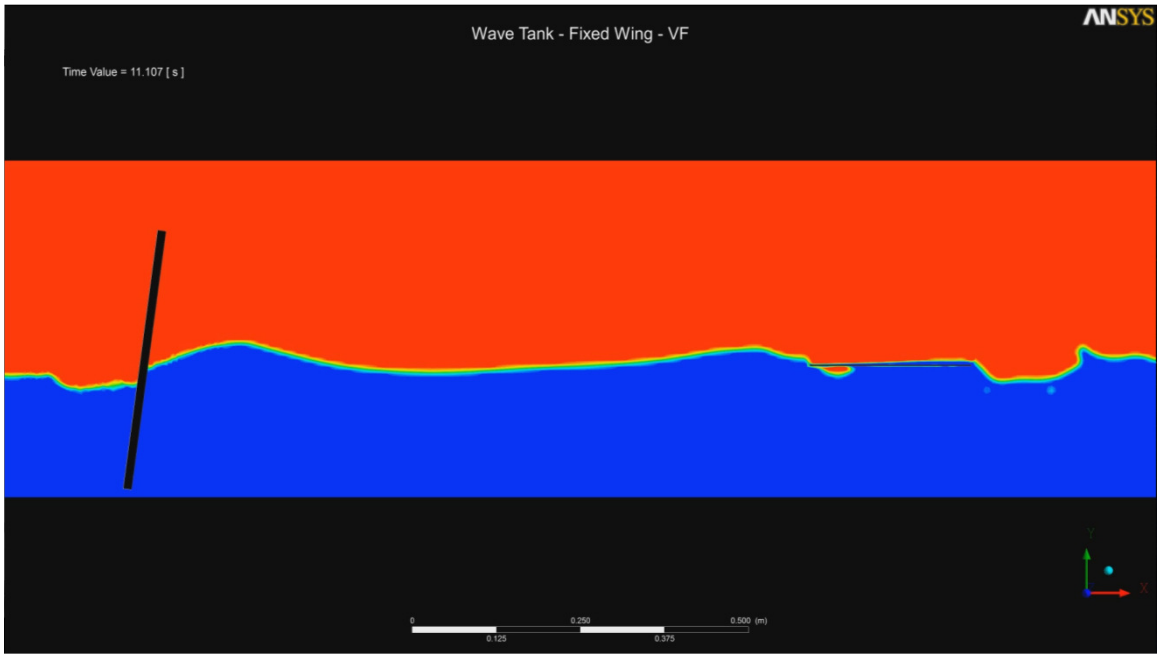

Wave Tank – Fixed Wing – VF.mp4

Fluid Flow – Moving Wing

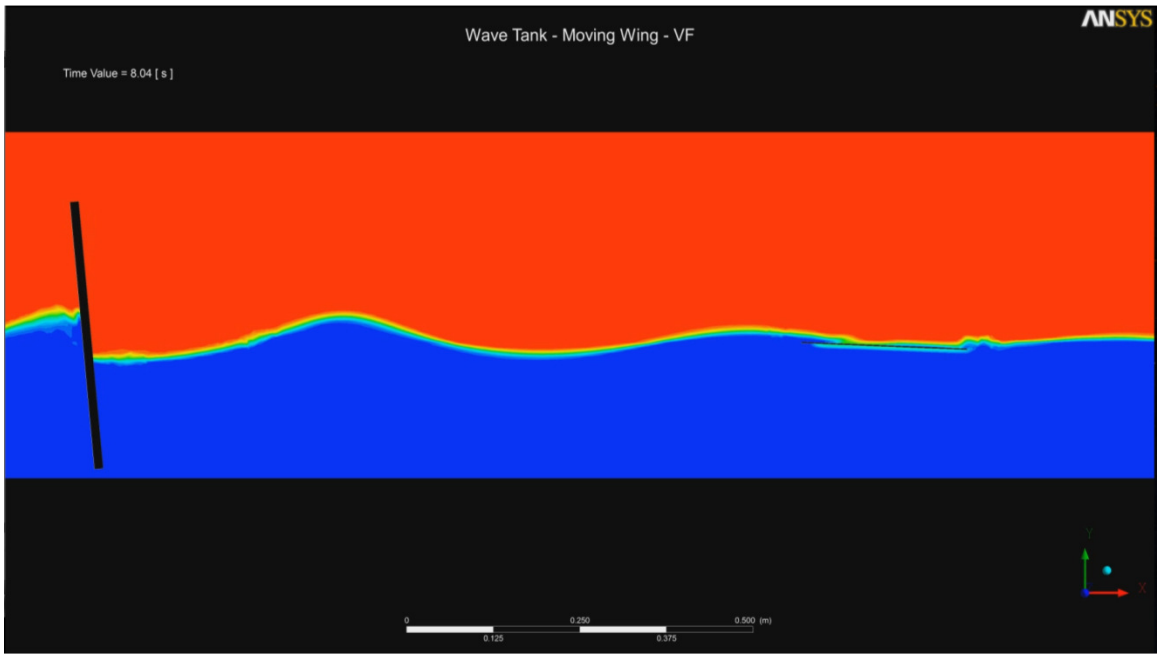

Wave Tank – Moving Wing – VF.mp4

Mesh Motion – Wave Generator

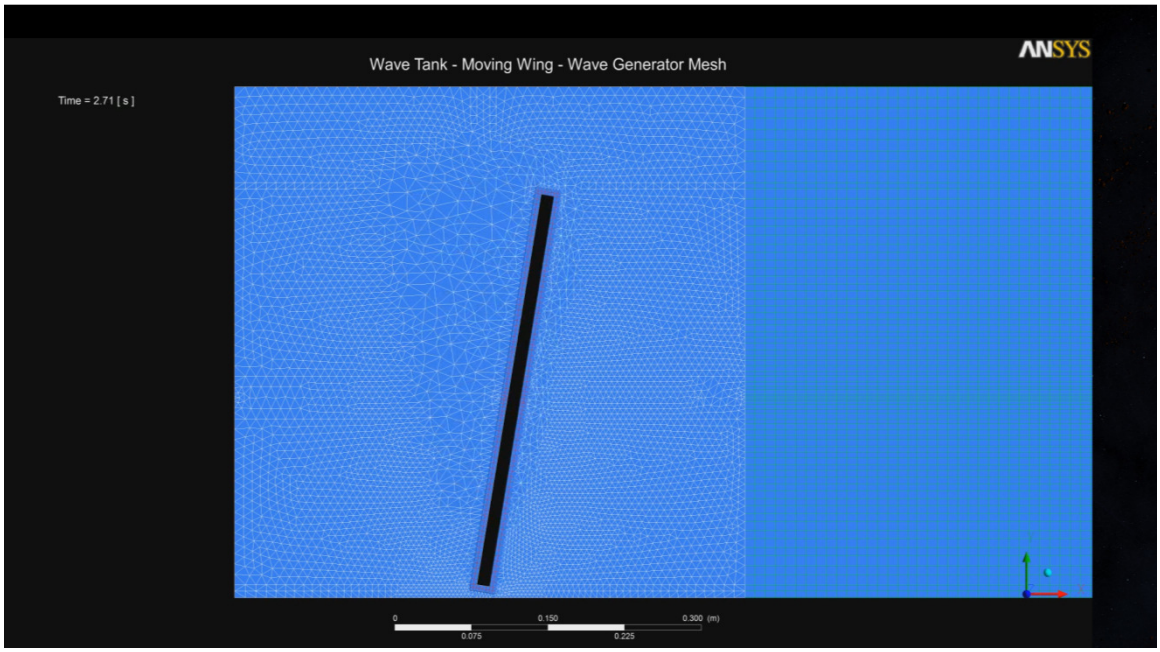

Wave Tank – WG Mesh Motion.mp4

Mesh Motion – Moving Wing

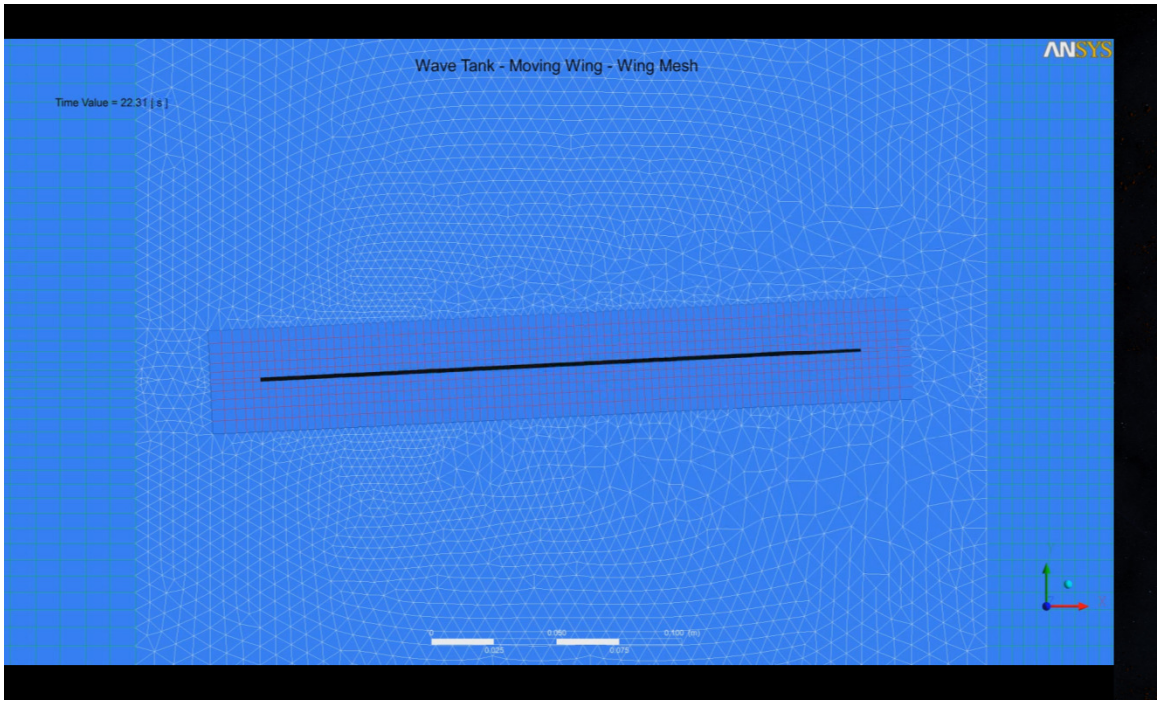

Wave Tank – Wing Mesh Motion.mp4

APPENDIX E:

SEA WALL ANIMATIONS

Fluid Flow

Model 1

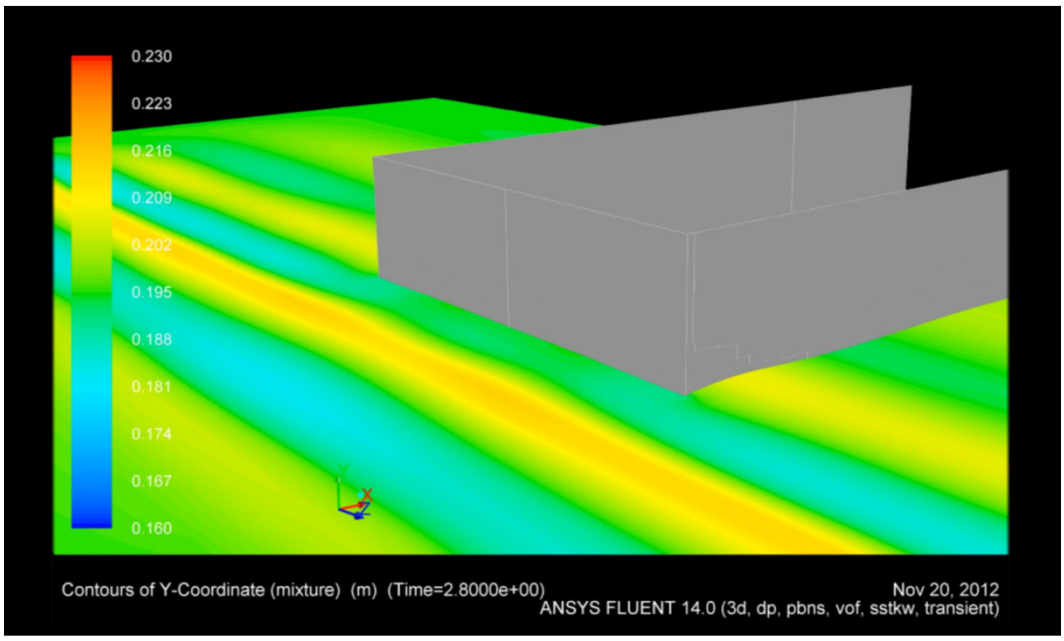

SW-V7-0deg-3W-1xA - VOF.mp4

Model 2

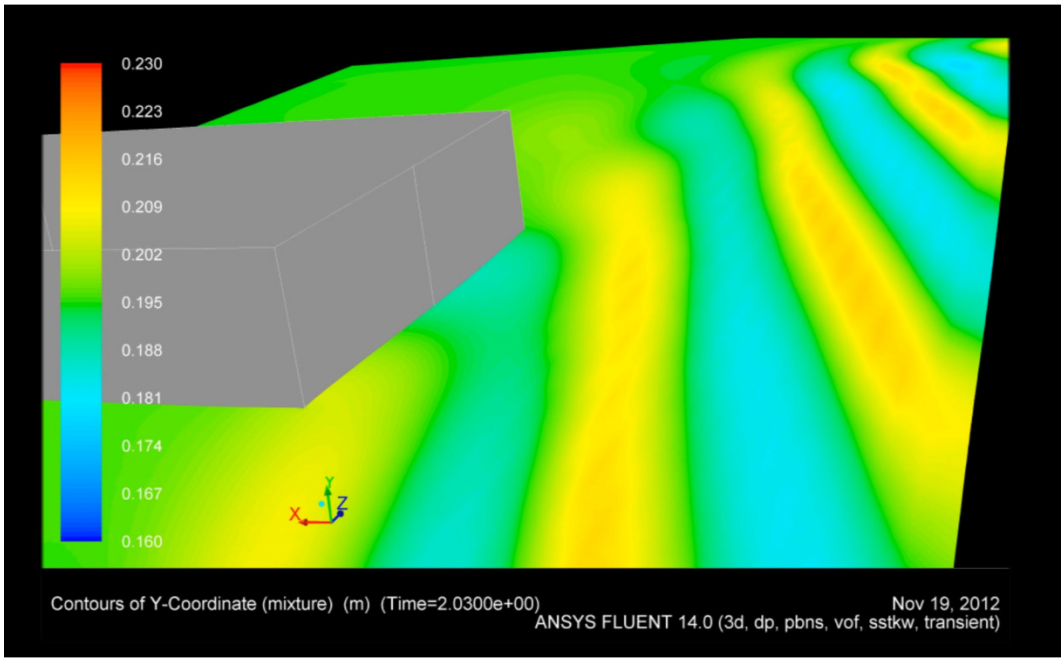

SW-V7-15deg-3W-1xA – VOF.mp4

Model 3

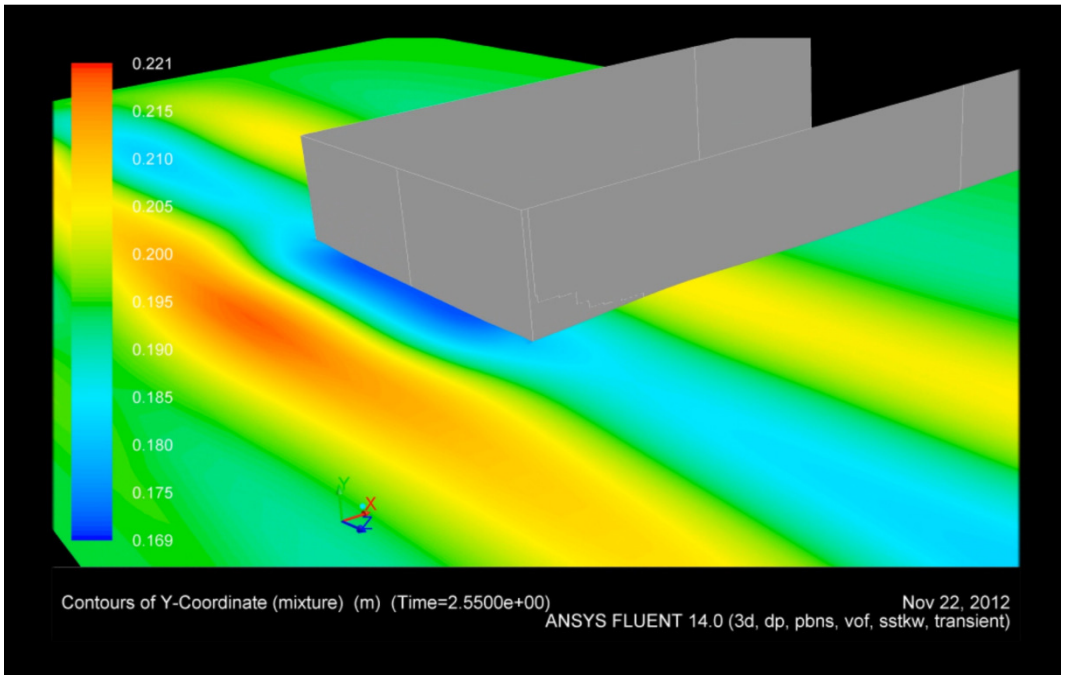

SW-V7-0deg-2W-Wave1 - VOF.mp4

Velocity YZ Plane – Right Corner

Model 1

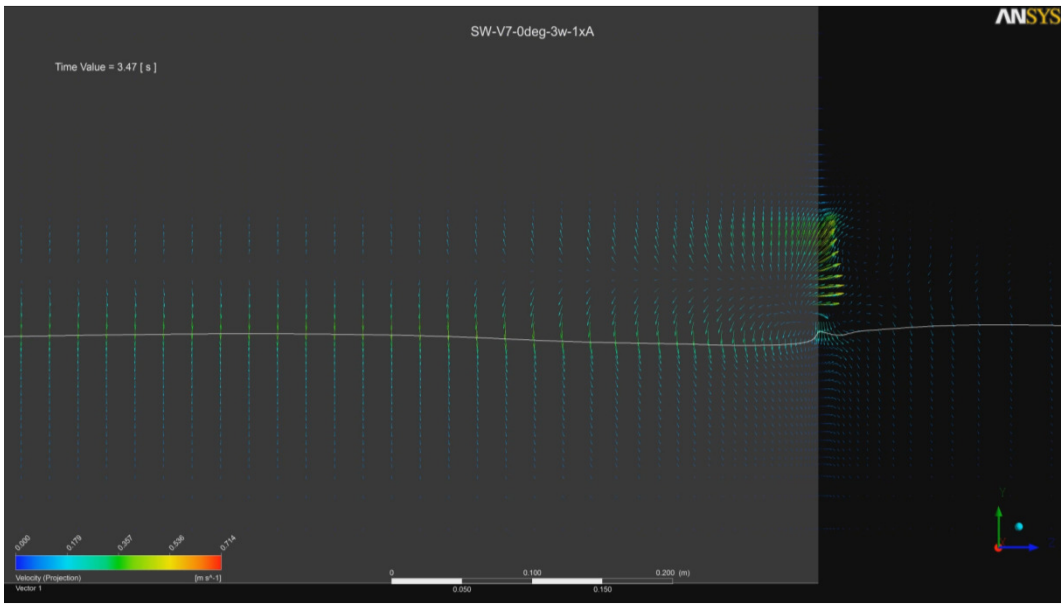

SW-V7-0deg-3W-1xA - YZ1.mp4

Model 2

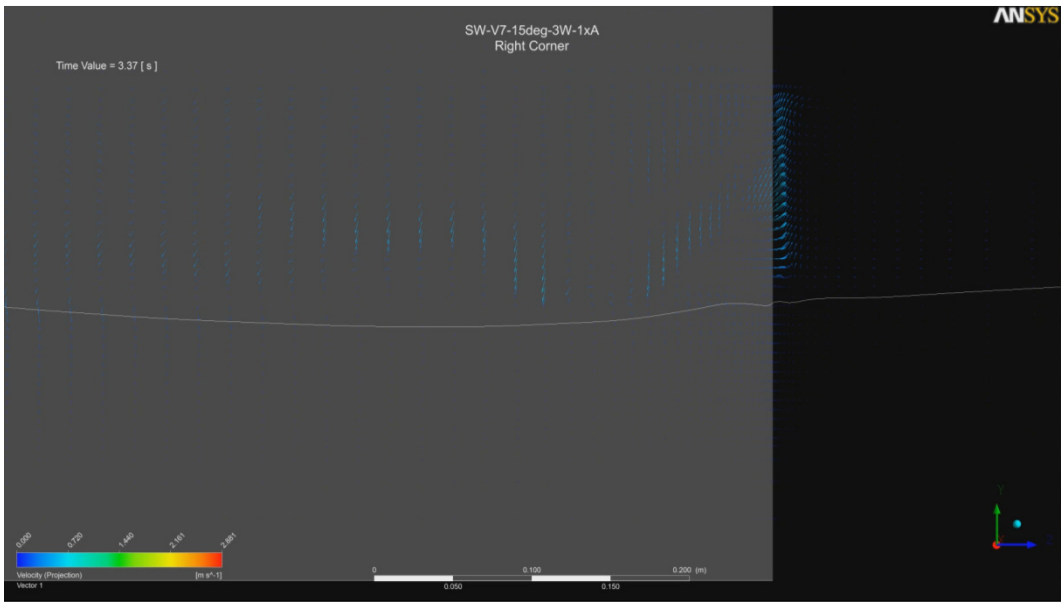

SW-V7-15deg-3W-1xA - YZ1 Right.mp4

Model 3

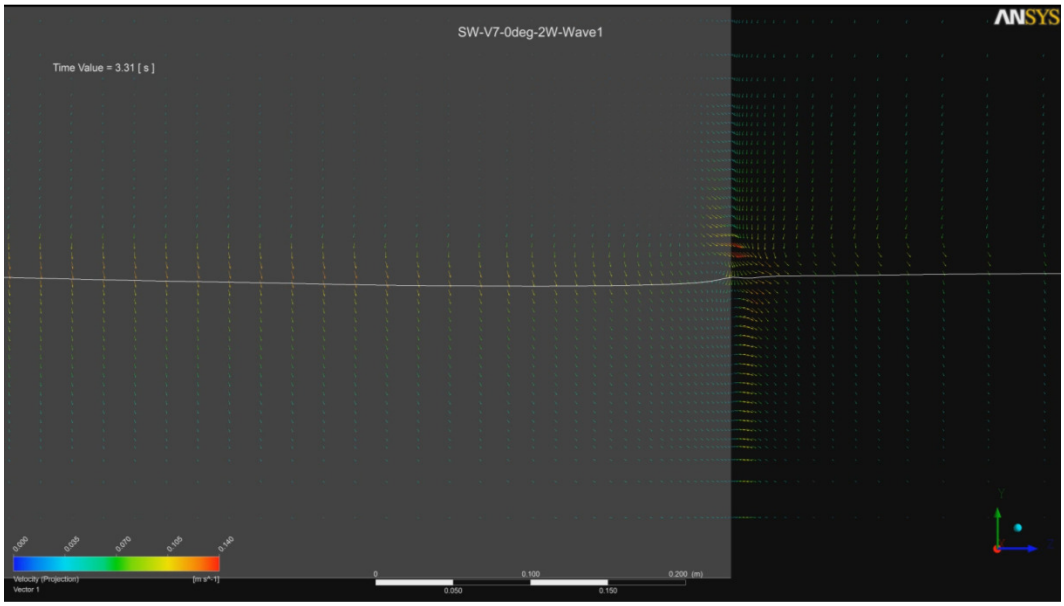

SW-V7-0deg-2W-Wave1 - YZ1.mp4

Velocity YZ Plane – Left Corner

Model 2

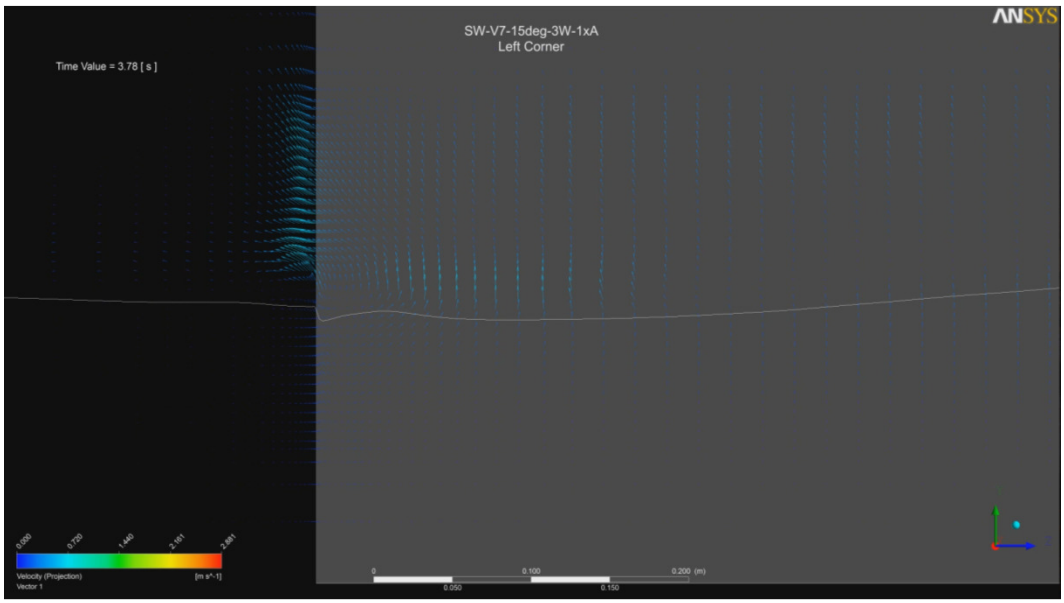

SW-V7-15deg-3W-1xA – YZ1 Right.mp4

Velocity Surface – Right Corner

Model 1

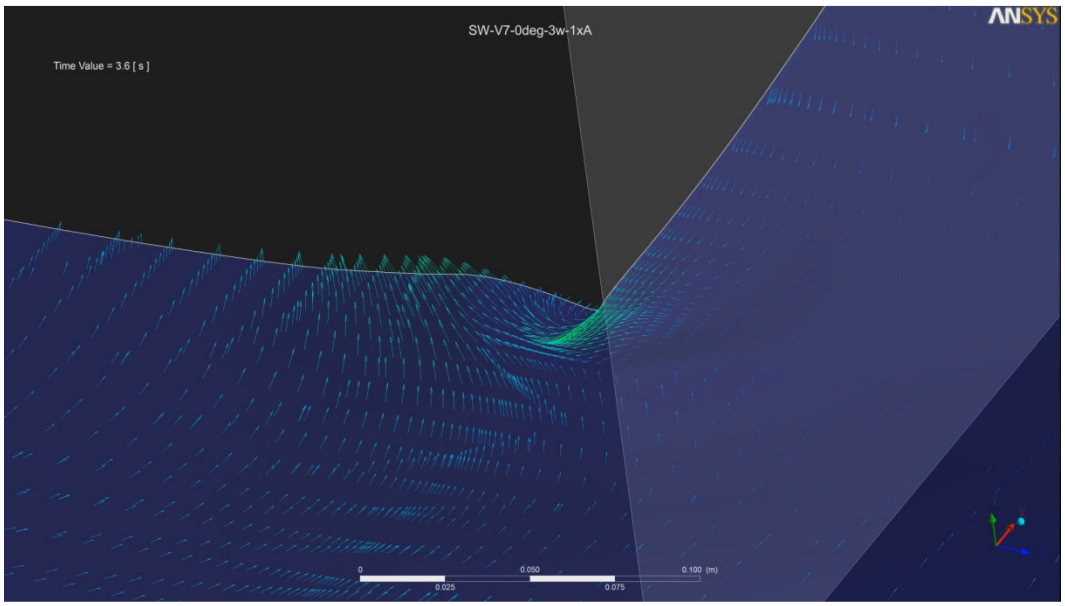

SW-V7-0deg-3W-1xA – RC Surface.mp4

Model 3

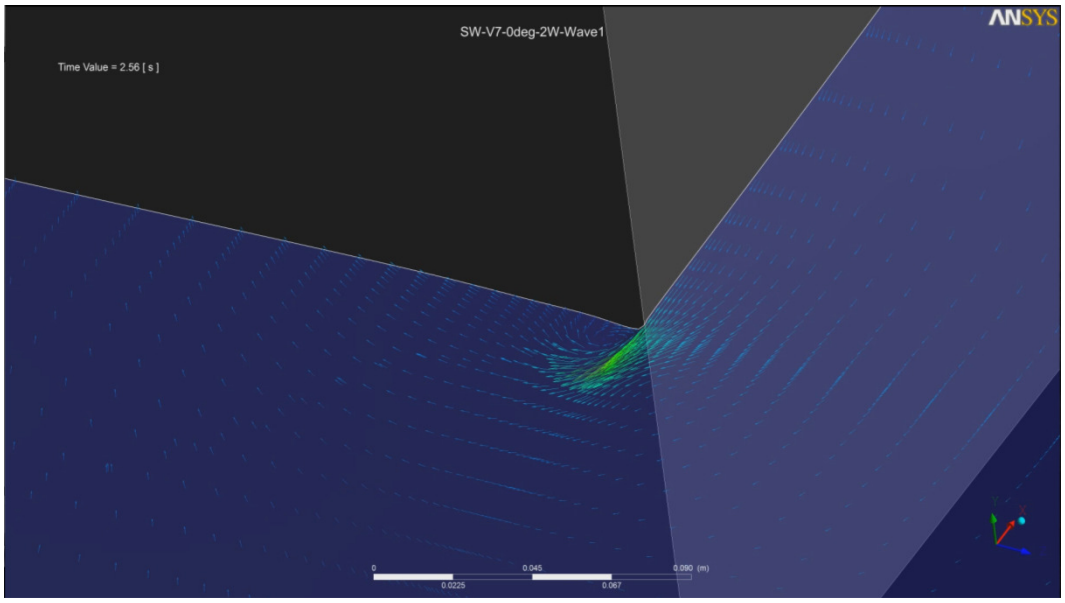

SW-V7-0deg-2W-Wave1 – RC Surface.mp4

Velocity Vortex – Right Corner

Model 1

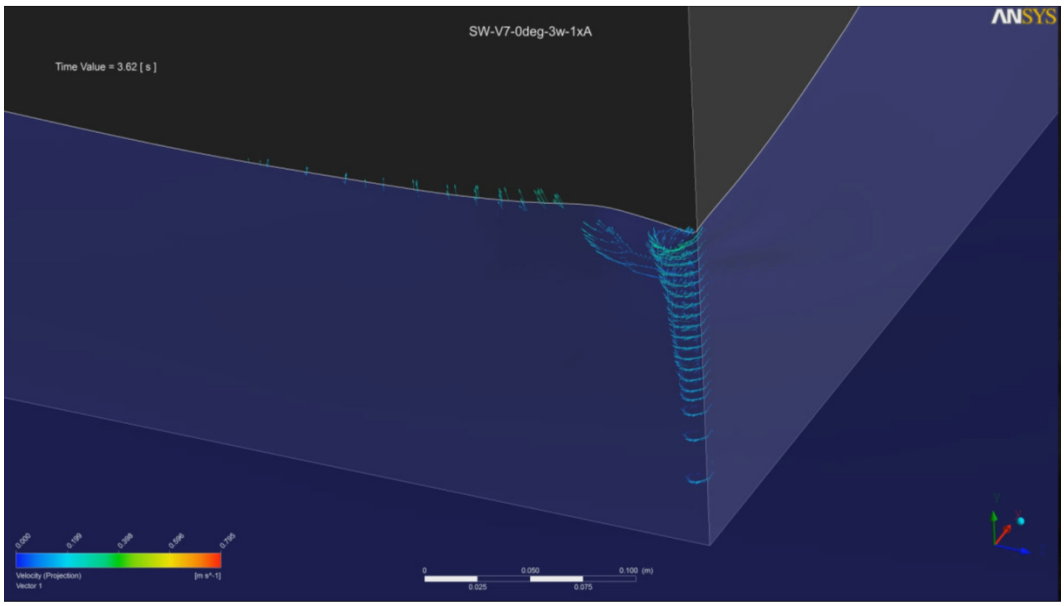

SW-V7-0deg-3W-1xA – RC Vortex.mp4

Velocity Vortex – Left Corner

Model 2

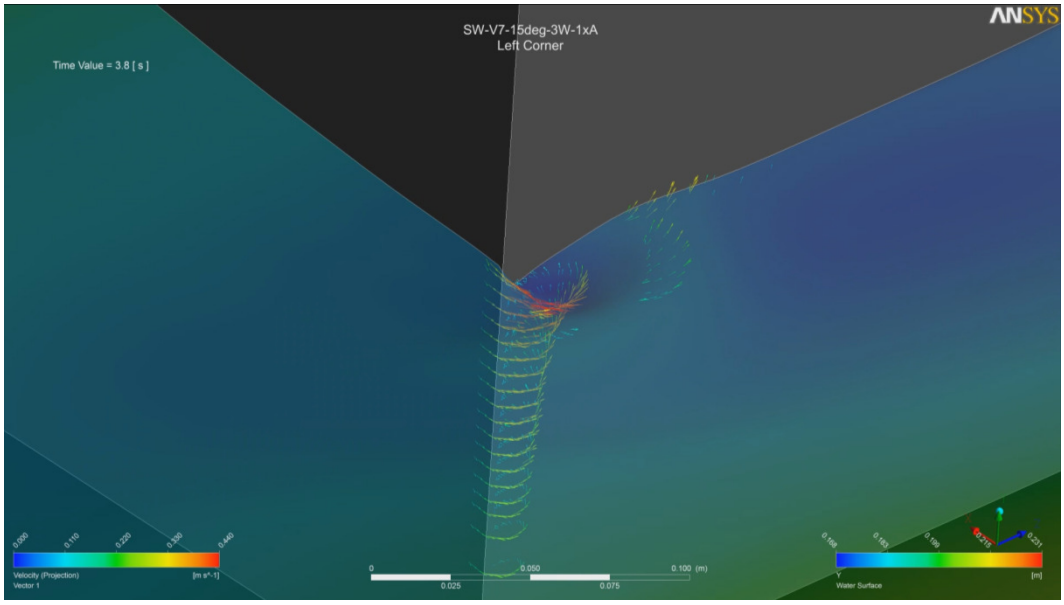

SW-V7-15deg-3W-1xA - LC Vortex.mp4